

Correspondent: David Ritson
Stanford Linear
Accelerator Center
P. O. Box 4349
Stanford, Calif. 94305

FTS/Commercial 415 - 854-3300 Ext. 2625
November, 1970

FOCUSING SPECTROMETER FACILITY

D. Ayers, R. Diebold, A. Greene, and A. Wicklund
Argonne National Laboratory

L. Guerriero
University of Bari

R. Lanou
Brown University

G. Cocconi, J. Litt
CERN

B. Gittelman, E. Loh
Cornell University

J. Friedman, H. Kendall, and L. Rosenson
Massachusetts Institute of Technology

A. E. Brenner, A. L. Read
National Accelerator Laboratory

R. Weinstein
Northeastern University

R. L. Anderson, K. L. Brown, D. Gustavson,
D. M. Ritson* and B. H. Wiik
Stanford University

ABSTRACT

It is proposed to build a strong focusing spectrometer. The spectrometer will be of flexible design and can operate either with 15μ steradians acceptance and $\pm 0.03\%$ momentum precision up to 200 GeV/c or can be changed to give considerably larger acceptances at lower momenta. The first proposed experiment is to measure elastic scattering and quasi two-body elastic scattering of K^+ , K^- , p , \bar{p} on hydrogen and deuterium (neutron) targets, up to 200 GeV/c and at $|t|$ values of 0 to $1.5(\text{GeV}/c)^2$.

*Coordinator

TABLE OF CONTENTS

	<u>Page</u>
Introduction	1
Proposed Experiment.	3
The Spectrometer Design and Optics	10
Instrumentation and Monitoring for the Beam and Spectrometer . .	14
Division of Responsibilities and Time Schedule	21
 Appendix 1: Differential Acromatic Cerenkov (DISC) Counter for NAL 200 GeV Beams	
 Appendix 2: Differential Cerenkov Counter for the Proposed 200 GeV Spectrometer	

INTRODUCTION

Focusing spectrometers have been built and operated at SLAC, CERN and elsewhere for the analysis of particle momenta up to ~ 25 GeV/c. We are proposing the construction of a focusing spectrometer for NAL that would measure the momenta of particles scattered from a target up to 200 GeV/c with very high precision. The instrument incorporates a number of features, of which some are adaptations from previous designs and some are novel.

1) It will be a strong focusing device capable of accepting 15μ steradians at 200 GeV/c and analyzing momenta to a precision of $\pm 0.03\%$ in $\Delta p/p$.

2) By moving the target closer to the spectrometer, or alternatively by repositioning the front quadrupole doublet, the acceptance will be considerably increased at lower energies.

3) The spectrometer will contain a region of high beam parallelism suitable for the introduction of high precision differential Cerenkov counters for mass determinations.

4) The input beam angle and production angle will be magnetically alterable over a wide angular range, while the spectrometer remains physically fixed in position.

5) If, as seems feasible, suitable momentum dispersion can be introduced into the primary input beam the spectrometer will operate in an "energy loss" mode. In this mode the final focus maps the energy loss in the target and full physics resolution is obtainable even with a very large spread ($\sim 1\%$) in the input beam momentum.

6) Detectors will be located in a well shielded environment 90 meters downstream from the target with counter planes of about 8 cm X 14 cm. Such a spectrometer should utilize not only the beam intensities available at switch on, but the considerably higher intensities that can be expected later in the accelerator's history.

The spectrometer components and length will be equivalent to about one-third those used for the main high precision 2.5 mr beam line and its construction should not be overly demanding. We expect the spectrometer and instrumentation to be used for many years in a set of developing programs.

The past record of spectrometer facilities has been good. Over the passage of years they have usually not only measured the original set of processes for which they were designed, but have probed both deeper and in more detail into the physics than was originally expected.

The areas of physics that can be investigated with such an instrument can be summarized as:

1) Elastic scattering processes in both the u and t channels.

2) Two-body quasi-elastic scattering processes such as $\pi^+ + P \rightarrow \pi^+ + N^{+*}$ where the resonance is produced via the exchange of a "pomeron".

3) Two-body and quasi two-body channels, involving the exchange of quantum numbers, such as $\pi^+ + P \rightarrow K^+ + \Sigma^+$.

4) Deeply inelastic processes such as $\pi^+ + P \rightarrow \pi^+ + \text{anything}$ and $K^+ + P \rightarrow K^+ + \text{anything}$.

5) Quark and exotic particle hunts. (We would hope to make some such hunts incidental to the line-up of the spectrometer.)

This proposal splits into two parts. First, we describe a proposed physics experiment which will serve as an excellent operational test of the facility. This first experiment is chosen a) for intrinsic physics interest, b) to be not too demanding so that even if the spectrometer is not performing with full capabilities initially the experiment can still be successfully carried to completion and c) to be hard to do by any other method.

Various groups in this collaboration will submit other separate proposals for different experiments to be done subsequently.

PROPOSED EXPERIMENT

We propose to measure $d\sigma/dt$ for the following set of reactions:

$$\begin{aligned} pp &\rightarrow pp \\ \bar{p}p &\rightarrow \bar{p}p \\ K^+p &\rightarrow K^+p \\ K^-p &\rightarrow K^-p \end{aligned}$$

We plan to do these experiments over an energy range from 50 GeV to 200 GeV and at t -values between 0 and $-1.5(\text{GeV}/c)^2$ as extensively as is possible within our time allocation. By use of the differential and threshold Cerenkov counters, p 's, K 's, and π 's can be simultaneously identified, permitting us in principle to collect data on three

reactions at the same time. We further plan to repeat some of these measurements with deuterium as a target to study the elastic scattering cross section on the neutron. Simultaneously with measuring the differential cross section for elastic scattering, we expect also to be able to study the cross sections for "diffractive" production up to missing masses of about 2 GeV. Previous experiments seem to indicate that several isobars have a total cross section nearly independent of energy and thus they should be accessible to measurements in this energy range.

After completion of the first experimental runs part of this collaboration will submit a proposal to extend these measurements.

Elastic Scattering

Elastic scattering processes are among the most studied, as well as among the least understood of all two-body reactions. We propose here to make a systematic study of K-nucleon, p-nucleon, as well as \bar{p} -nucleon scattering for energies between 50 and 200 GeV and for values of the four momentum transfer t from 0 out to about $-1.5(\text{GeV}/c)^2$. In the energy regions studied so far the cross sections for the various reactions have a rather different behaviour. The differential cross section for elastic pp scattering shows shrinkage but no structure for $|t|$ less than $1(\text{GeV}/c)^2$. This is in contrast to the behaviour of $\bar{p}p$ elastic scattering which has an expanding diffraction peak in addition to structure in the angular distribution around $-.6(\text{GeV}/c)^2$. The same disparity also exists in K-nucleon scattering; the differential cross section for K^+p has a smoothly shrinking t distribution, while K^-p has no shrinkage and a dip in the t

distribution for $t \sim -.8(\text{GeV}/c)^2$.

These features are generally explained within the framework of Reggeized particle exchange in the t-channel(1). In the t-channel all these reactions have the same quantum numbers and for energies up to 20 GeV the data can be fitted with the P , P' , ω , ρ , and A_2 trajectories. In the case of nucleon-nucleon scattering, the scattering amplitude can be schematically decomposed as follows:

$$A(pp) = P + P' - \omega - \rho + A_2$$

$$A(\bar{p}p) = P + P' + \omega + \rho + A_2$$

$$A(pn) = P + P' - \omega + \rho - A_2$$

$$A(\bar{p}n) = P + P' + \omega - \rho - A_2$$

From the fact that at high energies and small t-values the difference $\sigma(pp) - \sigma(pn)$ as well as the difference $\sigma(\bar{p}p) - \sigma(\bar{p}n)$ are both small it is generally concluded that the contribution from ρ and A_2 exchanges can be neglected. Therefore the observed differences between the pp cross section and the $\bar{p}p$ cross sections must be caused by ω -exchange, or written symbolically: $d\sigma/dt(pp) - d\sigma/dt(\bar{p}p) \sim \text{Im}\omega$. This would then imply that at the cross-over point, i.e., at the t-value where the two cross sections are equal, $\text{Im}\omega=0$. This can obviously be achieved by assuming that the residue of the ω trajectory has a dynamical zero and vanishes for this t-value. This assumption, however, leads to contradictions. In particular, we would then expect to see a dip in π^0 photoproduction for $t = -.2(\text{GeV}/c)^2$. Such a dip is not seen. By including absorption or cuts into the theories these

difficulties can be removed. The explanation in terms of pure t-channel exchanges is thus complex, and further experimentation over a wide range of variables is required before these processes are understood.

If the alternative viewpoint of "duality" is used, s-channel quantum numbers remain relevant at high energies(2). In the s-channel picture pp and $\bar{p}p$ as well as K^+p and K^-p have different quantum numbers and it is therefore not surprising that the s as well as the t dependences are different. In such a model we expect in general a cross section of the form:

$$\frac{d\sigma}{dt}(\bar{p}p) = P^2 + 2P J_0 + \dots$$

The contribution from the Pomeron is denoted by P and it is assumed that it only makes a contribution to the s-channel non-helicity-flip amplitude. J_0 is the contribution from the s-channel resonances. J_0 is expected to have maxima and minima as an ordinary 0-th order Bessel function as a function of t and in addition be dependent upon s.

Now in elastic processes with exotic quantum numbers in the s-channel, like pp or K^+p , there will be a contribution only from the Pomeron term, e.g., $d\sigma/dt(pp) = P^2$. Hence all the structure in the $\bar{p}p(K^-p)$ cross section at high energies must come from the interference term between the Pomeron and the resonances. The interference term can

be extracted from the ratio:

$$\frac{\frac{d\sigma}{dt}(\bar{p}p) - \frac{d\sigma}{dt}(pp)}{\sqrt{\frac{d\sigma}{dt}(pp)}} \sim J_0$$

We have evaluated this ratio at 8 and 16 GeV using the $\bar{p}p$ cross section from the recent data of Birnbaum et al.(3) and the pp cross sections from the experiment by Foley et al.(4). The result shown in Fig. 1 has some resemblance to a Bessel function $J_0(R\sqrt{E})$ with an interaction radius R of about 0.8 f. The cross-over point seems to move as a function of energy, but since we are using data from two different experiments this might simply be due to normalization errors. Since the cross-over point is strongly dependent upon the relative normalization it can only be determined in a meaningful way if both cross sections are determined with the same apparatus. Also a determination of the contribution from the ρ and A_2 trajectories can only be made by comparing (pp) with (pn) or $(\bar{p}p)$ with $(\bar{p}n)$ as measured with the same apparatus. It is a prediction common to all models that at high energies the differential cross sections for elastic scattering will all be dominated by the exchange of a single trajectory (the Pomeron) and thus the different reactions will have the same behaviour. Hence at the highest energies it is mandatory to measure the cross sections for (pp) , (pn) , $(\bar{p}p)$, and $(\bar{p}n)$ scattering using the same apparatus if we want to extract the differences between these processes in a reliable way and study how they approach this asymptotic limit.

The same remarks we have made about nucleon-nucleon scattering also apply to K-nucleon scattering. Again it is very important that

these cross sections are measured with the same apparatus in order to be able to extract the small differences between them in a quantitative way.

A check of systematic errors involved in extracting neutron cross sections from interactions in deuterium is conveniently provided by the charge symmetric relations

$$\frac{d\sigma}{dt}(\pi^+n) = \frac{d\sigma}{dt}(\pi^-p) ,$$

$$\frac{d\sigma}{dt}(\pi^-n) = \frac{d\sigma}{dt}(\pi^+p) .$$

Sufficient pion data will be collected simultaneously with the proton and kaon-data to make these checks as well as to compare normalizations with other experiments studying πp scattering.

Resonance Excitation

A high resolution single arm spectrometer is uniquely suited for the study of nucleon isobar production. The large mass acceptance of such an instrument permits measurement of isobar production up to about 2 GeV at the same time data is collected on the elastic channels. The high quality resolution is required to separate the isobars. At present there is only a limited amount of data available on isobar production at high energies. We propose here to measure the cross section for isobar production up to a missing mass of about 2 GeV using different incident particles. Previous experiments(5-13) show that at lower energies isobars at masses of 1238 MeV, 1410 MeV, 1518 MeV, 1688 MeV and at the highest energy 2119 MeV are excited. The t -dependences of these reactions are quite different. For the $N^*(1238)$ and the $N^*(1410)$ the slope is about $16(\text{GeV}/c)^2$ whereas the two other

isobars seem to have a slope of only $5(\text{GeV}/c)^2$. The $N^*(1410)$ and $N^*(1688)$ excitations seem to have constant cross sections over the whole energy range consistent with a quasi-diffractive behaviour, whereas the $N^*(1238)$ excitation drops off sharply. The $N^*(1518)$ excitations decrease rapidly with energy up to about 10 GeV and at higher energies shows an energy independent behaviour. In view of this remarkably different behaviour it is worthwhile to make a systematic study of these reactions at high energies. Such a study also permits a good check on factorization in the case of Pomeron exchange. According to this hypothesis the ratios

$$\frac{pp \rightarrow pN^*}{pp \rightarrow pp} = \frac{\pi p \rightarrow \pi N^*}{\pi p \rightarrow \pi p} = \frac{Kp \rightarrow KN^*}{Kp \rightarrow Kp}$$

should all be equal. Here N^* stands for any isobar that can be diffractively produced.

Time Estimate

To carry out this program about 800 experimental hours are needed. In addition we request about 200 hours for checking out the apparatus previous to the run. Table 2 gives a breakdown of the expected time allocations to the various parts of the experiment. This time estimate has been based upon 3×10^{12} protons per pulse incident on the production target. As an example, Tables 3 and 4 show the expected rates for $\bar{p}p \rightarrow \bar{p}p$ and $K^-p \rightarrow K^-p$ as functions of incident energies and t -values.

THE SPECTROMETER DESIGN AND OPTICS

The spectrometer will occupy a fixed location and will disperse particles in the horizontal plane. Changes of scattering angle will be introduced by magnetically steering the input beam. The layout is shown schematically in Fig. 2 and consist of a quad pair focusing a point object to a parallel beam followed by bend magnets and differential Cerenkov counters. The beam will then be reimaged to a point focus by a final quadrupole doublet. The length of the system will be about 130 meters. Twenty meters of 10 cm bore quadrupoles and twenty-four meters of standard NAL bend magnets will be required to construct the system. A rough measure of the complexity of the spectrometer can be obtained by comparing it to the 2.5 mr high precision input beam. The input beam is 400 meters long, will have three cross-over foci. Instead of the one focus of the spectrometer and will require about twice the amount of components.

Considerable studies have been made by us as to the most economical design for the spectrometer. We believe the proposed design to be the most economical method for doing the physics in which we are interested.

The solid angle acceptance will be increased at low energies by moving the front quads closer to the target, or alternatively by moving the target (and input beam focus) closer to the spectrometer. Either method of increasing the solid angle should be relatively simple. Fig. 3 shows the physical layout of the spectrometer in the Meson Laboratory.

Table 1 gives the rough parameters of the system. Tables 5 and 6 give "transport" runs for a specimen high energy configuration capable of measuring up to 200 GeV/c with 15μ steradians acceptance, and for a 60 GeV configuration with a 40μ steradian acceptance. Table 7 gives the required alignment tolerances of the various components. The only stringent requirements for the spectrometer are on the lateral misplacements of the quads, and on the field precisions required for the quads. The physical alignment precisions are not excessive. The proposed 10 cm bore quads are expected to have fields good to .1% on the pole tips. This is adequate for our design.

Use of Spectrometer in an Energy Loss Mode

If the spectrometer is fed with an input beam with a horizontal momentum dispersion matched to that of the spectrometer, the spectrometer will operate as an energy loss spectrometer. In this mode of operation, particles that do not suffer any energy loss in the target will be momentum recombined at the final spectrometer focus. Those suffering an energy loss will be focused to an appropriately displaced image. As an example of operation in this mode consider a process such as:

$$\pi^+ + P \rightarrow K^+ + \Sigma^+$$

With an input beam having an energy of 100 GeV and a momentum bite as high as 1% the spectrometer could still determine the missing mass of the " Σ^+ " to better than 50 MeV.

In principle it is relatively simple to alter the

magnification of the 2.5 mr beam to achieve the required dispersion. Further investigation will be required to establish how easy this will be in practice, given the relatively "frozen" specifications for this beam.

Decode Planes and Accuracy of Determination of Experimental Parameters

Table 8 shows the transfer matrices from the target to the various decode planes for the 200 GeV/c configuration. One of the elegant properties of a focusing spectrometer is the high "magnification" that can generally be found for any specific parameter at some point of a well designed system. For instance at vertical plane 1, the vertical input height is magnified by a factor 13. By linear combinations of the planes we will be able to measure the horizontal and vertical production angles, the momentum (or energy loss) of the particle, and the vertical production point.

Input Beam Steering and Scattering Angle Variation

Figs. 4A and 4B show two methods that can be used to vary the scattering angle. The system in Fig. 4A will consist of 3 meters of bend magnets placed before and after the target. The first bend magnet will bend the input beam down and the second bend magnet, after the target, will steer the scattered particles back onto the spectrometer axis. Such a system will introduce up to 3 GeV/c transverse momentum at high energies. The system in Fig. 4B shows a 3 meter pre-bend magnet placed 27 meters upstream of the target and a 9 meter bend magnet placed just before the target. The main deflection is produced by the magnet just before the target. It will be possible by re-rigging the bend magnets for either system to introduce either

vertical (orthogonal to the bend plane) or horizontal deflections.

Primary Beam Dump and Background Problems

It is proposed to dump the input beam into a beam dump just ahead of the first quadrupole pair.

The main counting systems should be almost totally unaffected by background from the beam dump as they will start 90 meters downstream from the dump point, will have dimensions of the order 8 cm X 13 cm, and will be protected by 2 meters of bend magnet. The only point at which trouble could occur will be at the differential Cerenkov counter located after 3 meters of bend magnet behind the first quadrupole pairs. If this counter counted in excess of 10^7 particles per second we would be in trouble. However, this counter is located thirty meters distant from the dump point, and because of its special properties of very high directivity and high specificity of mass selection we do not envisage any severe background problems. It is worth noting that the location for the differential Cerenkov counter, with the spectrometer operated in a pair "energy loss" mode, would be after all the bend magnets. Therefore, even with the very high input beam intensities possible in such a mode, the Cerenkov counter would be in a very well protected location.

Spectrometer Alignment

Spectrometer alignment would proceed through four phases:

1. Accurate magnetic measurements of individual components.
2. Transit survey and alignment of the components in place.

3. Use of the precision input beam spot to delineate the beam axis and foci of the system.

4. Exploration of the aperture of the spectrometer by sweeping the input beam across the spectrometer.

All these types of measurement have been made routinely in the past on SLAC and other spectrometers to the required precisions.

Costs of the Magnetic System

Table 9 lists components and estimated costs.

INSTRUMENTATION AND MONITORING FOR THE BEAM AND THE SPECTROMETER

The detector systems for the beam and spectrometer will contain the following elements:

- 1) DISC Cerenkov counters in the beam to identify the mass of the input beam particles, and differential as well as threshold Cerenkov counters placed in the spectrometer to identify the outgoing particles.
- 2) Trigger scintillators to provide, along with the Cerenkov counters, an interrogation pulse.
- 3) Charpak proportional counters placed in the spectrometer to ascertain the momentum and scattering angles of the detected particles.
- 4) A crude scintillator hodoscope close to the target to provide coplanarity and some angular information.
- 5) A monitor system to determine the intensity and the phase space of the input beam.

- 6) A data collection system capable of both "housekeeping" the equipment and providing an immediate "physics" answer.
- 7) A liquid hydrogen target.
- 8) Shower and interaction counters to identify electrons and muons.

We discuss these items in detail below.

Mass Discrimination

The best instruments for providing mass separation at high momenta are the differential Cerenkov counters and the UV threshold Cerenkov counter. The most taxing requirement is to be able to separate pions from K mesons at the highest momenta. The DISC Cerenkov counter described in Appendix 1 is limited in solid angle but is ideal placed in the beam line for identification of beam particles, in particular those that represent a small fraction of the particles in the beam. The differential Cerenkov counter described in Appendix 2 permits larger angular spreads in the beam and will be used with the spectrometer.

Our second tool to provide particle separation is the UV threshold Cerenkov counter developed at Serpukhov. One of these counters will be placed between the last quadrupole and the focal plane, the second after the focal plane. Each counter will be about 25 meters long. At high energies where there are few photoelectrons available we will add the signals. At lower energies they can be used as two separate counters. At 100 GeV/c an absolute pressure of 70 mm of Hg for hydrogen gas is required to put K mesons at threshold, in which case 50 meters constitute 0.75×10^{-3} radiation lengths and a

negligible amount of multiple scattering. The Prokoshkin group (IHEP preprint 69-63) have obtained

$$N_e = 160 \theta^2 L$$

where N_e is the number of photoelectrons in a 56 UVP photomultiplier, θ is the Cerenkov angle in radians, and L is the active length in centimeters. With the counter set to K threshold

$$N_e = .036 \left(\frac{L}{10}\right) \left(\frac{100 \text{ GeV/c}^2}{p}\right)^2$$

for pions, giving about 18 photoelectrons from 50 meters of counter at 100 GeV/c. At 200 GeV/c, this becomes 4.5 photoelectrons, leading to a probability for no signal of about 10^{-2} .

One DISC Cerenkov counter will be located in the primary beam, one differential counter will be located in the parallel beam region after three meters of bend magnet and one at the end of the bend section.

Trigger Scintillators

The main interrogation trigger for the system will probably consist of $\check{C}_B - C_1 - C_2 - S_1$, where S_1 will be a scintillator either before the last quadrupole pair, or at the momentum plane. \check{C}_B will be the beam Cerenkov counter, C_1 will be the first differential counter, and C_2 will be the second differential counter. The system will thus require few scintillators to provide the trigger pulse. We will probably only use \check{C}_B for less frequent particles like \bar{p} and K's in

order to take advantage of the full beam intensity.

Charpak Proportional Counters

On receipt of an interrogation signal we will interrogate eight Charpak planes located along the last sixty meters of the spectrometer. Because of the focusing properties of the spectrometer these planes will not be larger than 8 cm X 14 cm, and thus with a 1 mm wire spacing, will only contain a total of about 1,000 wires. In order to decode the particle trajectories and momenta, (c.f. Table 8) only the horizontal planes H1, H2, and the vertical planes V1 and V3 are required. H3 and V2 will be redundant horizontal and vertical planes and H'2 and V'2 will be two redundant planes rotated at $+45^\circ$ and -45° to the vertical.

The poorer time resolution of the Charpak chambers relative to scintillators should not be a problem as backgrounds are expected to be low in the focal plane region. The 1 mm chamber wire spacing should provide ~ 0.5 mm resolution.

Recoil Particle Detector

For elastic scattering, detection of the recoil proton near the target will provide us with a coplanarity check and possibly angular information. In principle, this information is redundant but in practice it may be of considerable help in the early stages of the experiment. A rather small number of strip counters parallel to the target axis are all that are required to define the coplanarity.

If possible we will also include two hodoscope planes separated by one meter to measure the production angles. Such a hodoscope would become increasingly useful at high t -values, where the

relationship between the laboratory angle of the recoil proton and the t -value is given by $\sin \theta = (1 + |t|/4m^2)^{-1/2}$. The angular system would be designed to measure the angle of the recoil proton to about 10 mr (F.W.H.M.). This measurement of the proton will determine dt/t to about 5×10^{-2} for t larger than $0.5(\text{GeV}/c)^2$.

Beam Flux Determination

The incident beam flux monitors must handle from 10^6 to about 10^{10} particles per second. For total flux determinations of instantaneous rates below 10^7 per second a simple scintillator telescope in the incident beam is sufficient. As an additional independent monitoring system, we plan to use a high pressure gas Cerenkov counter. For instantaneous rates above 10^7 per second the high pressure gas counter will be modified so that the total anode current of the phototube can be measured. A suitably designed system would yield an anode current of about 0.05 mA for a beam intensity of 10^{10} per second. With a correction for dark current this device can be used over the entire range required, including absolute calibration against a counter at 10^7 particles per second. The calibration constant is sensitive to proton velocity and is expected to vary by about 4% in a known way for protons over 5 GeV/c. As a second incident beam monitor, above the range where individual beam particles can be counted, we will install a thin scattering target (about 0.1 g/cm^2) in the beam. In counter telescopes set off to the side of the beam we would expect a counting rate of about 100 per second for an incident beam of 10^6 /second, a counting rate of 10^6 /second for an incident beam of 10^{10} protons/second.

The DISC Cerenkov counter will be satisfactory for monitoring particles that make up only a small fraction of the incident beam, such as K mesons.

Beam Position Monitors

It is important that beam steering changes can be quickly and conveniently detected. By switching off the input beam deflecting magnets so that the spectrometer sits at 0^0 the relative momentum calibrations and beam alignment can be rapidly determined. However it will be important to determine that conditions have remained constant during an experimental data run.

We will install beam position monitors in crucial places along the beam line, in particular, just before the hydrogen target. ZnS screens will not be satisfactory in all cases because of the low beam intensity. Several types of monitors are being considered and probably more than one type will be used since different ones will work best at different intensities. The monitors will be remotely retractable. We also plan to insert hodoscopes in the beam to determine the phase space of the beam at the target.

Data Collection System and Preprocessor

One of the advantages of a "spectrometer" setup is that it performs a continuing group of experiments over an extended period. It is therefore worth the effort to provide a system of data processing that not only housekeeps but provides almost fully analyzed data on-line, leaving only the final detailed small corrections to be made off-line. The input information to the computer will be contained in the trigger pulse, information from the threshold counters, pulse

height analyzers, the coordinates from the eight Charpak planes encoded as six eight bit numbers, and hodoscope information accounting for an additional three eight bit numbers. A typical input event will therefore consist of 100 to 200 bits.

The operations to be performed on this information will require about twenty multiplications and additions per event to extract momenta, production angles, and perform coplanarity and redundancy checks. Randomly sampled "raw" events will be accumulated on tape for both analyzed and ambiguous events so that reliable efficiencies can be subsequently determined.

Every attempt will be made to have a system that will "immediately" detect physics features of interest and that will permit instant cross checks to determine whether they are valid, or whether they result from instrumental artifacts.

Hydrogen Target

The target can be of modest design and can be cooled by a local refrigerator unit as is now common practice in this application. The target will have provision for several cells, including hydrogen, deuterium and empty cells.

Miscellaneous Instrumentation

We will build an NMR system to read the magnetic fields in all the bend magnets remotely and continuously with high accuracy.

A light pulser system will be built for preliminary line-up of counters.

DIVISION OF RESPONSIBILITIES AND TIME SCHEDULE

Counting, monitor equipment and interfacing to be provided by the user groups.

Magnets, power supplies, mechanical installation, liquid hydrogen target, and computer to be provided by NAL. Table 9 lists the magnetic components and estimated costs.

Table 10 shows a breakdown of the equipment to be provided by the users groups.

Time Schedule

Provided we get a "green light" to proceed we would expect to have the magnetic system specified by February 1971, components delivered by December 1971, and in place by March 1972. We would expect to have the counting equipment and detectors available for test and installation at this time, and to be ready to test and check out the system by June 1972.

REFERENCES

For a recent review of the data and the different theoretical models see:

- 1) J.D. Jackson, Proceedings of the Lund International Conference on Elementary Particles 1969.
- 2) H. Harari, SLAC-PUB-821.
- 3) Birnbaum et al., Phys. Rev. Letters 23, 663 (1969).
- 4) Foley et al., Phys. Rev. Letters 11, 425 (1963).
- 5) G. Cocconi et al., Phys. Rev. Letters 7, 450 (1961).
- 6) G. B. Chadwick et al., Phys. Rev. 128, 1823 (1962).
- 7) G. Cocconi et al., Phys. Letters 8, 134 (1964).
- 8) G. Bellettini et al., Phys. Letters 18, 167 (1965).
- 9) E. W. Anderson et al., Phys. Rev. Letters 16, 855 (1966).
- 10) I. M. Blair et al., Phys. Rev. Letters 17, 789 (1966).
- 11) K. J. Foley et al., Phys. Rev. Letters 19, 397 (1967).
- 12) C. M. Ankenbrandt et al., Phys. Rev. 170, 1223 (1968).
- 13) J. V. Allaby et al., Phys. Letters 28B, 67 (1968).

TABLE 1

Design Parameters of Focusing Spectrometer for the
Meson Laboratory

Momentum resolution at 200 GeV/c	$\delta p/p = \pm 0.032\%$
Solid angle acceptance at: 200 GeV/c 60 GeV/c	$\sim 15\mu$ steradians $\sim 40\mu$ steradians
Maximum angular divergence through differential Cerenkov at 200 GeV/c	$\Delta\theta = \pm 0.2$ mrad
Momentum acceptance	$\Delta p/p = 4\%$ (F.W.)
Momentum dispersion	3cms per %
Angular resolution	$\pm .1$ mrad
Maximum intensity beam	$\sim 10^{10} - 10^{11}$ /pulse
Maximum momentum	200 GeV/c
Method of production angle variation	Magnetic bending of beam
Incident spot size	1mm (F.W.)

TABLE 2

Estimates of Time in Hours Required for the Experiment

Energy (GeV) Reaction	50		75		100		125		150		175		Total time for reaction
	t(GeV ²)	Time	t(GeV ²)	Time	t(GeV ²)	Time	t(GeV ²)	Time	t(GeV ²)	Time	t(GeV ²)	Time	
pp → pp	0-1.0	10	0-1.0	10	0-1.0	10	0-1.0	10	0-1.0	10	0-1.0	10	60
pp → pn*	0-1.0	10	0-1.0	10	0-1.0	10	0-1.0	10	0-1.0	10	0-1.0	10	60
pn → pn	0-1.0	10	0-1.0	10	0-1.0	10	0-1.0	10	0-1.0	10	0-1.0	10	60
$\bar{p}p \rightarrow \bar{p}p$	0-1.0	15	0-1.0	15	0-1.0	20	0-1.0	30	0-1.5	20			100
$\bar{p}n \rightarrow \bar{p}n$	0-1.0	15	0-1.0	15									30
$K^+p \rightarrow K^+p$	0-1.5	20	0-1.5	30	0-1.5	40	0-1.2	40	0-1.0	30			160
$K^+p \rightarrow K^+N^*$	0-1.5	10	0-1.5	10	0-1.5	15							25
$K^+n \rightarrow K^+n$	0-1.0	10	0-1.0	10	0-1.0	15							35
$K^-p \rightarrow K^-p$	0-1.5	20	0-1.5	30	0-1.5	40	0-1.2	40	0-1.0	30			160
$K^-p \rightarrow K^-N^*$	0-1.5	10	0-1.5	10	0-1.5	15							25
$K^-n \rightarrow K^-n$	0-1.0	10	0-1.0	10	0-1.0	15							35

TABLE 3

Expected Rates for $\bar{p}p \rightarrow \bar{p}p$

t GeV ²	E GeV	\bar{p} ⁽¹⁾	Counts hr.	E GeV	\bar{p} ⁽¹⁾	Counts hr.	E GeV	\bar{p} ⁽¹⁾	Counts hr.	E GeV	\bar{p} ⁽¹⁾	Counts hr.	Counts ⁽²⁾ hr.
.0	50	7×10^5	5.0×10^6	75	2×10^5	2.2×10^6	100	5×10^4	7.2×10^5	125	8×10^3	1.4×10^5	1.1×10^4
.1	"	"	1.5×10^6	"	"	6.4×10^5	"	"	2.2×10^5	"	"	4.4×10^4	3.3×10^3
.2	"	"	4.6×10^5	"	"	2.0×10^5	"	"	6.5×10^4	"	"	1.3×10^4	9.8×10^2
.3	"	"	1.4×10^5	"	"	6.0×10^4	"	"	1.9×10^4	"	"	3.9×10^3	2.9×10^2
.4	"	"	4.2×10^4	"	"	1.8×10^4	"	"	5.9×10^3	"	"	1.2×10^3	8.9×10
.5	"	"	1.3×10^4	"	"	5.6×10^3	"	"	1.8×10^3	"	"	3.6×10^2	2.7×10
.6	"	"	3.8×10^3	"	"	1.6×10^3	"	"	5.4×10^2	"	"	1.1×10^2	8.1
.7	"	"	1.1×10^3	"	"	4.7×10^2	"	"	1.6×10^2	"	"	3.2×10	2.4
.8	"	"	3.4×10^2	"	"	1.5×10^2	"	"	4.8×10	"	"	9.6	.7
.9	"	"	1.0×10^2	"	"	4.3×10^1	"	"	1.4×10	"	"	2.9	.22
1.0	"	"	3.0×10^1	"	"	1.3×10^1	"	"	4.4	"	"	.9	.07

(1) Number of \bar{p} 's per pulse in 1% $\Delta p/p$.(2) Assumed .5m long liquid hydrogen target and $d\sigma/dt = 80(\text{mb}/\text{GeV}^2) \cdot e^{12t}$.

TABLE 4

Expected Rates for $K^- p \rightarrow K^- p$

t GeV ²	E_0 GeV	K^- (1)	Counts hr.	(2)	E_0 GeV	K^- (1)	Counts hr.	(2)	E_0 GeV	K^- (1)	Counts hr.	(2)	E_0 GeV	K^- (1)	Counts hr.	(2)
.0	50	4 X 10 ⁶	5.9 X 10 ⁶	6	75	7 X 10 ⁵	1.6 X 10 ⁶	5	100	2 X 10 ⁵	6.1 X 10 ⁵	5	125	4 X 10 ⁴	1.5 X 10 ⁵	4
.1	"	"	3.0 X 10 ⁶	6	"	"	8.0 X 10 ⁵	5	"	"	3.0 X 10 ⁵	4	"	"	7.5 X 10 ⁴	3
.2	"	"	1.5 X 10 ⁶	6	"	"	4.0 X 10 ⁵	5	"	"	1.5 X 10 ⁵	4	"	"	3.8 X 10 ⁴	3
.3	"	"	7.5 X 10 ⁵	5	"	"	2.0 X 10 ⁵	4	"	"	7.5 X 10 ⁴	4	"	"	1.9 X 10 ⁴	3
.4	"	"	3.7 X 10 ⁵	5	"	"	9.7 X 10 ⁴	4	"	"	3.7 X 10 ⁴	3	"	"	9.3 X 10 ³	3
.5	"	"	1.8 X 10 ⁵	5	"	"	4.8 X 10 ⁴	4	"	"	1.8 X 10 ⁴	3	"	"	4.6 X 10 ³	2
.6	"	"	9.2 X 10 ⁴	4	"	"	2.4 X 10 ⁴	4	"	"	9.2 X 10 ³	3	"	"	2.3 X 10 ³	2
.7	"	"	4.1 X 10 ⁴	4	"	"	1.2 X 10 ⁴	4	"	"	4.6 X 10 ³	3	"	"	1.1 X 10 ³	2
.8	"	"	2.3 X 10 ⁴	4	"	"	6.0 X 10 ³	3	"	"	2.3 X 10 ³	2	"	"	5.7 X 10 ²	2
.9	"	"	1.1 X 10 ⁴	3	"	"	2.9 X 10 ³	3	"	"	1.1 X 10 ³	2	"	"	2.8 X 10 ²	2
1.0	"	"	5.6 X 10 ³	3	"	"	1.5 X 10 ³	2	"	"	5.6 X 10 ²	2	"	"	1.4 X 10 ²	2
1.1	"	"	2.8 X 10 ³	3	"	"	7.3 X 10 ²	2	"	"	2.8 X 10 ²	2	"	"	6.9 X 10	8.3
1.2	"	"	1.4 X 10 ³	3	"	"	3.6 X 10 ²	2	"	"	1.4 X 10 ²	2	"	"	3.4 X 10	4.1
1.3	"	"	6.8 X 10 ²	2	"	"	1.8 X 10 ²	2	"	"	6.8 X 10	2	"	"	1.7 X 10	2.1
1.4	"	"	3.4 X 10 ²	2	"	"	8.4 X 10	2	"	"	3.4 X 10	2	"	"	8.5	1.0
1.5	"	"	1.7 X 10 ²	2	"	"	4.4 X 10	2	"	"	1.7 X 10	2	"	"	4.3	.5

(1) Number of K^- 's per pulse in 1% $\Delta p/p$.(2) Assumed .5m long liquid hydrogen target and $d\sigma/dt = 17(\text{mb/GeV}^2) : e^{7t}$.

NAL200 GEV/C SPECTROMETER WITH STANDARD ELEMENTS 29 NOV 70

```

*BEAM*      1.000000  200.00 GEV
             0.0 M      0.0      0.050 CM
                   0.0      1.150 MR      0.0
                   0.0      0.050 CM      0.0      0.0
                   0.0      4.010 MR      0.0      0.0      0.0
                   0.0      0.0 CM      0.0      0.0      0.0      0.0
                   0.0      2.000 PC      0.0      0.0      0.0      0.0      0.0

*DRIFT*      3.0      7.0000 M
             7.0 M      0.0      0.807 CM
                   0.0      1.150 MR      0.998
                   0.0      2.807 CM      0.0      0.0
                   0.0      4.010 MR      0.0      0.0      1.000
                   0.0      0.0 CM      0.0      0.0      0.0      0.0
                   0.0      2.000 PC      0.0      0.0      0.0      0.0      0.0

*QUAD*      5.00      1.52000 M  -10.4323 KG  5.000 CM  ( -20.785 M )
            LABEL = Q1
             8.5 M      0.0      1.012 CM
                   0.0      1.579 MR      0.999
                   0.0      3.309 CM      0.0      0.0
                   0.0      2.548 MR      0.0      0.0      1.000
                   0.0      0.0 CM      0.0      0.0      0.0      0.0
                   0.0      2.000 PC      0.0      0.0      0.0      0.0      0.0

*DRIFT*      3.0      0.5000 M
             9.0 M      0.0      1.091 CM
                   0.0      1.579 MR      0.999
                   0.0      3.436 CM      0.0      0.0
                   0.0      2.548 MR      0.0      0.0      1.000
                   0.0      0.0 CM      0.0      0.0      0.0      0.0
                   0.0      2.000 PC      0.0      0.0      0.0      0.0      0.0

*QUAD*      5.00      1.52000 M  -10.4323 KG  5.000 CM  ( -20.785 M )
            LABEL = Q1
             10.5 M      0.0      1.374 CM
                   0.0      2.162 MR      1.000
                   0.0      3.695 CM      0.0      0.0
                   0.0      0.844 MR      0.0      0.0      0.998
                   0.0      0.0 CM      0.0      0.0      0.0      0.0
                   0.0      2.000 PC      0.0      0.0      0.0      0.0      0.0

*DRIFT*      3.0      0.5000 M
             11.0 M      0.0      1.482 CM
                   0.0      2.162 MR      1.000
                   0.0      3.737 CM      0.0      0.0
                   0.0      0.844 MR      0.0      0.0      0.998
                   0.0      0.0 CM      0.0      0.0      0.0      0.0
                   0.0      2.000 PC      0.0      0.0      0.0      0.0      0.0

```

QUAD 5.00 1.52000 M -10.4323 KG 5.000 CM (-20.785 M)
 LABEL = Q1
 12.6 M 0.0 1.868 CM
 0.0 2.953 MR 1.000
 0.0 3.730 CM 0.0 0.0
 0.0 0.945 MR 0.0 0.0 -0.998
 0.0 0.0 CM 0.0 0.0 0.0 0.0
 0.0 2.000 PC 0.0 0.0 0.0 0.0 0.0

DRIFT 3.0 0.5000 M
 13.1 M 0.0 2.016 CM
 0.0 2.953 MR 1.000
 0.0 3.682 CM 0.0 0.0
 0.0 0.945 MR 0.0 0.0 -0.998
 0.0 0.0 CM 0.0 0.0 0.0 0.0
 0.0 2.000 PC 0.0 0.0 0.0 0.0 0.0

QUAD 5.00 1.52000 M -10.4323 KG 5.000 CM (-20.785 M)
 LABEL = Q1
 14.6 M 0.0 2.544 CM
 0.0 4.030 MR 1.000
 0.0 3.408 CM 0.0 0.0
 0.0 2.640 MR 0.0 0.0 -1.000
 0.0 0.0 CM 0.0 0.0 0.0 0.0
 0.0 2.000 PC 0.0 0.0 0.0 0.0 0.0

DRIFT 3.0 1.5000 M
 16.1 M 0.0 3.148 CM
 0.0 4.030 MR 1.000
 0.0 3.013 CM 0.0 0.0
 0.0 2.640 MR 0.0 0.0 -1.000
 0.0 0.0 CM 0.0 0.0 0.0 0.0
 0.0 2.000 PC 0.0 0.0 0.0 0.0 0.0

QUAD 5.00 1.52000 M 7.5459 KG 5.000 CM (29.337 M)
 LABEL = Q2
 17.6 M 0.0 3.673 CM
 0.0 2.852 MR 1.000
 0.0 2.687 CM 0.0 0.0
 0.0 1.665 MR 0.0 0.0 -0.999
 0.0 0.0 CM 0.0 0.0 0.0 0.0
 0.0 2.000 PC 0.0 0.0 0.0 0.0 0.0

DRIFT 3.0 0.5000 M
 18.1 M 0.0 3.816 CM
 0.0 2.852 MR 1.000
 0.0 2.604 CM 0.0 0.0
 0.0 1.665 MR 0.0 0.0 -0.999
 0.0 0.0 CM 0.0 0.0 0.0 0.0
 0.0 2.000 PC 0.0 0.0 0.0 0.0 0.0

QUAD 5.00 1.52000 M 7.5459 KG 5.000 CM (29.337 M)
 LABEL = Q2
 19.6 M 0.0 4.147 CM

0.0	1.477	MR	1.000					
0.0	2.417	CM	0.0	0.0				
0.0	0.807	MR	0.0	0.0	-0.995			
0.0	0.0	CM	0.0	0.0	0.0	0.0		
0.0	2.000	PC	0.0	0.0	0.0	0.0	0.0	0.0

DRIFT 3.0 0.5000 M

20.1 M	0.0	4.220	CM					
	0.0	1.477	MR	1.000				
	0.0	2.377	CM	0.0	0.0			
	0.0	0.807	MR	0.0	0.0	-0.995		
	0.0	0.0	CM	0.0	0.0	0.0	0.0	
	0.0	2.000	PC	0.0	0.0	0.0	0.0	0.0

QUAD 5.00 1.52000 M 7.5459 KG 5.000 CM (29.337 M)

LABEL = Q2

21.6 M	0.0	4.333	CM					
	0.0	0.013	MR	0.024				
	0.0	2.317	CM	0.0	0.0			
	0.0	0.087	MR	0.0	0.0	0.015		
	0.0	0.0	CM	0.0	0.0	0.0	0.0	
	0.0	2.000	PC	0.0	0.0	0.0	0.0	0.0

DRIFT 3.0 1.0000 M

22.6 M	0.0	4.333	CM					
	0.0	0.013	MR	0.025				
	0.0	2.317	CM	0.0	0.0			
	0.0	0.087	MR	0.0	0.0	0.019		
	0.0	0.0	CM	0.0	0.0	0.0	0.0	
	0.0	2.000	PC	0.0	0.0	0.0	0.0	0.0

BEND 4.000 3.05000 M 16.000 KG 0.0000 (0.419 D)

LABEL = B1

25.7 M	0.0	4.333	CM					
	0.0	0.147	MR	0.002				
	0.0	2.317	CM	0.0	0.0			
	0.0	0.087	MR	0.0	0.0	0.030		
	0.0	0.032	CM	-1.000	0.001	0.0	0.0	
	0.0	2.000	PC	0.005	0.996	0.0	0.0	-0.002

DRIFT 3.0 20.0000 M

45.7 M	0.0	4.344	CM					
	0.0	0.147	MR	0.070				
	0.0	2.329	CM	0.0	0.0			
	0.0	0.087	MR	0.0	0.0	0.104		
	0.0	0.032	CM	-0.997	0.001	0.0	0.0	
	0.0	2.000	PC	0.072	0.996	0.0	0.0	-0.002

TRANSFORM 1

2.16789	3.76619	0.0	0.0	0.0	0.15743
-0.26552	-0.00001	0.0	0.0	0.0	0.07315
0.0	0.0	-4.86166	0.57763	0.0	0.0
0.0	0.0	-1.73119	-0.00000	0.0	0.0

-0.02004	-0.02755	0.0	0.0	1.00000	-0.00003
0.0	0.0	0.0	0.0	0.0	1.00000

END*	4.000	6.10000 M	16.000 KG	0.0000 (0.838 D)		
	LABEL = B2						
	51.8 M	0.0	4.360 CM				
		0.0	0.439 MR	0.109			
		0.0	2.335 CM	0.0	0.0		
		0.0	0.087 MR	0.0	0.0	0.127	
		0.0	0.095 CM	-0.999	-0.056	0.0	0.0
		0.0	2.000 PC	0.113	1.000	0.0	0.0
							-0.061

DRIFT	3.0	0.5000 M					
	52.3 M	0.0	4.362 CM				
		0.0	0.439 MR	0.114			
		0.0	2.336 CM	0.0	0.0		
		0.0	0.087 MR	0.0	0.0	0.128	
		0.0	0.095 CM	-0.998	-0.056	0.0	0.0
		0.0	2.000 PC	0.118	1.000	0.0	0.0
							-0.061

BEND	4.000	6.10000 M	16.000 KG	0.0000 (0.838 D)		
	LABEL = B2						
	58.4 M	0.0	4.417 CM				
		0.0	0.731 MR	0.193			
		0.0	2.343 CM	0.0	0.0		
		0.0	0.087 MR	0.0	0.0	0.151	
		0.0	0.159 CM	-0.995	-0.094	0.0	0.0
		0.0	2.000 PC	0.197	1.000	0.0	0.0
							-0.099

DRIFT	3.0	0.5000 M					
	58.9 M	0.0	4.424 CM				
		0.0	0.731 MR	0.201			
		0.0	2.344 CM	0.0	0.0		
		0.0	0.087 MR	0.0	0.0	0.152	
		0.0	0.159 CM	-0.994	-0.094	0.0	0.0
		0.0	2.000 PC	0.205	1.000	0.0	0.0
							-0.099

BEND	4.000	6.10000 M	16.000 KG	0.0000 (0.838 D)		
	LABEL = B2						
	65.0 M	0.0	4.562 CM				
		0.0	1.023 MR	0.312			
		0.0	2.352 CM	0.0	0.0		
		0.0	0.087 MR	0.0	0.0	-0.174	
		0.0	0.224 CM	-0.985	-0.141	0.0	0.0
		0.0	2.000 PC	0.316	1.000	0.0	0.0
							-0.146

DRIFT	3.0	0.5000 M					
	65.5 M	0.0	4.578 CM				
		0.0	1.023 MR	0.322			
		0.0	2.353 CM	0.0	0.0		
		0.0	0.087 MR	0.0	0.0	0.176	
		0.0	0.224 CM	-0.983	-0.141	0.0	0.0
		0.0	2.000 PC	0.327	1.000	0.0	0.0
							-0.146

BEND 4.000 3.05000 M 16.000 KG 0.0000 (0.419 D)
 LABEL = B2
 68.5 M 0.0 4.697 CM
 0.0 1.169 MR 0.385
 0.0 2.358 CM 0.0 0.0
 0.0 0.087 MR 0.0 0.0 0.187
 0.0 0.257 CM -0.975 -0.169 0.0 0.0
 0.0 2.000 PC 0.389 1.000 0.0 0.0 -0.174

DRIFT 3.0 1.0000 M
 69.5 M 0.0 4.743 CM
 0.0 1.169 MR 0.406
 0.0 2.360 CM 0.0 0.0
 0.0 0.087 MR 0.0 0.0 0.190
 0.0 0.257 CM -0.969 -0.169 0.0 0.0
 0.0 2.000 PC 0.410 1.000 0.0 0.0 -0.174

QUAD 5.00 1.52000 M 5.6038 KG 5.000 CM (39.415 M)
 VARY CODE = 020000
 LABEL = Q3
 71.1 M 0.0 4.725 CM
 0.0 1.282 MR -0.547
 0.0 2.408 CM 0.0 0.0
 0.0 0.629 MR 0.0 0.0 0.991
 0.0 0.257 CM -0.961 0.759 0.0 0.0
 0.0 2.000 PC 0.441 0.509 0.0 0.0 -0.174

DRIFT 3.0 0.5000 M
 71.6 M 0.0 4.691 CM
 0.0 1.282 MR -0.538
 0.0 2.439 CM 0.0 0.0
 0.0 0.629 MR 0.0 0.0 0.991
 0.0 0.257 CM -0.957 0.759 0.0 0.0
 0.0 2.000 PC 0.451 0.509 0.0 0.0 -0.174

QUAD 5.00 1.52000 M 5.6038 KG 5.000 CM (39.415 M)
 VARY CODE = 020000
 LABEL = Q3
 73.1 M 0.0 4.499 CM
 0.0 2.146 MR -0.851
 0.0 2.582 CM 0.0 0.0
 0.0 1.266 MR 0.0 0.0 0.998
 0.0 0.257 CM -0.946 0.975 0.0 0.0
 0.0 2.000 PC 0.484 0.048 0.0 0.0 -0.174

DRIFT 3.0 0.5000 M
 73.6 M 0.0 4.408 CM
 0.0 2.146 MR -0.844
 0.0 2.645 CM 0.0 0.0
 0.0 1.266 MR 0.0 0.0 0.998
 0.0 0.257 CM -0.942 0.975 0.0 0.0
 0.0 2.000 PC 0.495 0.048 0.0 0.0 -0.174

VARY CODE = C30000

82.2 M

0.0	3.093	CM						
0.0	1.814	MR	0.428					
0.0	3.371	CM	0.0	0.0				
0.0	1.336	MR	0.0	0.0	-0.999			
0.0	0.257	CM	-0.756	0.267	0.0	0.0		
0.0	2.000	PC	0.776	0.902	0.0	0.0		-0.174

DRIFT

3.0

25.0000 M

107.2 M

0.0	6.491	CM						
0.0	1.814	MR	0.903					
0.0	0.152	CM	0.0	0.0				
0.0	1.336	MR	0.0	0.0	-0.176			
0.0	0.257	CM	-0.174	0.267	0.0	0.0		
0.0	2.000	PC	1.000	0.902	0.0	0.0		-0.174

TRANSFORM 1

-1.47314	0.00000	0.0	0.0	0.0	0.0	3.24546
-0.72763	-0.67880	0.0	0.0	0.0	0.0	0.81828
0.0	0.0	-3.04863	-0.00000	0.0	0.0	0.0
0.0	0.0	4.71684	-0.32801	0.0	0.0	0.0
-0.11561	-0.22030	0.0	0.0	1.00000	-0.02242	
0.0	0.0	0.0	0.0	0.0	1.00000	

IT* 10.0 -1. 2. 0.0 / 0.000

0.000

FIT 10.0 -3. 4. 0.0 / 0.000

-0.000

DRIFT

3.0

25.0000 M

132.2 M

0.0	10.762	CM						
0.0	1.814	MR	0.966					
0.0	3.317	CM	0.0	0.0				
0.0	1.336	MR	0.0	0.0	0.999			
0.0	0.257	CM	0.008	0.267	0.0	0.0		
0.0	2.000	PC	0.983	0.902	0.0	0.0		-0.174

LENGTH

132.1596 M

TABLE 6

96-34

NAL60 GEV/C SPECTROMETER WITH STANDARD ELEMENTS 29 NOV 70

```

*PEAM*      1.000000    60.00 GEV
             0.0 M      0.0      0.050 CM
                       0.0      1.550 MR      0.0
                       0.0      0.050 CM      0.0      0.0
                       0.0      5.830 MR      0.0      0.0      0.0
                       0.0      0.0 CM      0.0      0.0      0.0      0.0
                       0.0      2.000 PC      0.0      0.0      0.0      0.0      0.0

*DRIFT*      3.0      5.1000 M
             5.1 M      0.0      0.792 CM
                       0.0      1.550 MR      0.998
                       0.0      2.974 CM      0.0      0.0
                       0.0      5.830 MR      0.0      0.0      1.000
                       0.0      0.0 CM      0.0      0.0      0.0      0.0
                       0.0      2.000 PC      0.0      0.0      0.0      0.0      0.0

*QUAD*      5.00      1.52000 M      -9.4806 KG      5.000 CM ( -6.697 M )
             LABEL = Q1
             6.6 M      0.0      1.124 CM
                       0.0      2.904 MR      1.000
                       0.0      3.508 CM      0.0      0.0
                       0.0      1.079 MR      0.0      0.0      0.997
                       0.0      0.0 CM      0.0      0.0      0.0      0.0
                       0.0      2.000 PC      0.0      0.0      0.0      0.0      0.0

*DRIFT*      3.0      1.0000 M
             7.6 M      0.0      1.415 CM
                       0.0      2.904 MR      1.000
                       0.0      3.616 CM      0.0      0.0
                       0.0      1.079 MR      0.0      0.0      0.997
                       0.0      0.0 CM      0.0      0.0      0.0      0.0
                       0.0      2.000 PC      0.0      0.0      0.0      0.0      0.0

*QUAD*      5.00      1.52000 M      -9.4806 KG      5.000 CM ( -6.697 M )
             LABEL = Q1
             9.1 M      0.0      2.030 CM
                       0.0      5.340 MR      1.000
                       0.0      3.385 CM      0.0      0.0
                       0.0      4.060 MR      0.0      0.0      -1.000
                       0.0      0.0 CM      0.0      0.0      0.0      0.0
                       0.0      2.000 PC      0.0      0.0      0.0      0.0      0.0

*DRIFT*      3.0      1.0000 M
             10.1 M      0.0      2.564 CM
                       0.0      5.340 MR      1.000
                       0.0      2.979 CM      0.0      0.0
                       0.0      4.060 MR      0.0      0.0      -1.000
                       0.0      0.0 CM      0.0      0.0      0.0      0.0
                       0.0      2.000 PC      0.0      0.0      0.0      0.0      0.0

```

QUAD 5.00 1.52000 M 5.3559 KG 5.000 CM (12.549 M)
 LABEL = Q2
 11.7 M 0.0 3.202 CM
 0.0 2.970 MR 1.000
 0.0 2.535 CM 0.0 0.0
 0.0 1.841 MR 0.0 0.0 -0.998
 0.0 0.0 CM 0.0 0.0 0.0 0.0
 0.0 2.000 PC 0.0 0.0 0.0 0.0 0.0

DRIFT 3.0 1.0000 M
 12.7 M 0.0 3.499 CM
 0.0 2.970 MR 1.000
 0.0 2.352 CM 0.0 0.0
 0.0 1.841 MR 0.0 0.0 -0.998
 0.0 0.0 CM 0.0 0.0 0.0 0.0
 0.0 2.000 PC 0.0 0.0 0.0 0.0 0.0

QUAD 5.00 1.52000 M 5.3559 KG 5.000 CM (12.549 M)
 LABEL = Q2
 14.2 M 0.0 3.727 CM
 0.0 0.021 MR -0.004
 0.0 2.214 CM 0.0 0.0
 0.0 0.132 MR 0.0 0.0 0.016
 0.0 0.0 CM 0.0 0.0 0.0 0.0
 0.0 2.000 PC 0.0 0.0 0.0 0.0 0.0

DRIFT 3.0 1.0000 M
 15.2 M 0.0 3.727 CM
 0.0 0.021 MR -0.004
 0.0 2.214 CM 0.0 0.0
 0.0 0.132 MR 0.0 0.0 0.021
 0.0 0.0 CM 0.0 0.0 0.0 0.0
 0.0 2.000 PC 0.0 0.0 0.0 0.0 0.0

BEND 4.000 3.05000 M 4.800 KG 0.0000 (0.419 D)
 LABEL = B1
 18.2 M 0.0 3.727 CM
 0.0 0.148 MR 0.001
 0.0 2.215 CM 0.0 0.0
 0.0 0.132 MR 0.0 0.0 0.040
 0.0 0.027 CM -1.000 0.003 0.0 0.0
 0.0 2.000 PC 0.006 0.990 0.0 0.0 -0.002

DRIFT 3.0 20.0000 M
 38.2 M 0.0 3.739 CM
 0.0 0.148 MR 0.080
 0.0 2.241 CM 0.0 0.0
 0.0 0.132 MR 0.0 0.0 0.157
 0.0 0.027 CM -0.997 0.003 0.0 0.0
 0.0 2.000 PC 0.084 0.990 0.0 0.0 -0.002

TRANSFORM 1
 1.67123 2.40310 0.0 0.0 0.0 0.15743

-0.41612	0.00000	0.0	0.0	0.0	0.07315
0.0	0.0	-7.02211	0.37964	0.0	0.0
0.0	0.0	-2.63405	0.00000	0.0	0.0
-0.01878	-0.01758	0.0	0.0	1.00000	-0.00003
0.0	0.0	0.0	0.0	0.0	1.00000

BEND 4.000 6.10000 M 4.800 KG 0.0000 (0.838 D)

LABEL = B2

44.3 M	0.0	3.758 CM					
	0.0	0.439 MR	0.127				
	0.0	2.255 CM	0.0	0.0			
	0.0	0.132 MR	0.0	0.0	0.191		
	0.0	0.082 CM	-0.998	-0.066	0.0	0.0	
	0.0	2.000 PC	0.131	0.999	0.0	0.0	-0.070

DRIFT 3.0 0.5000 M

44.8 M	0.0	3.760 CM					
	0.0	0.439 MR	0.133				
	0.0	2.256 CM	0.0	0.0			
	0.0	0.132 MR	0.0	0.0	0.194		
	0.0	0.082 CM	-0.998	-0.066	0.0	0.0	
	0.0	2.000 PC	0.137	0.999	0.0	0.0	-0.070

BEND 4.000 6.10000 M 4.800 KG 0.0000 (0.838 D)

LABEL = B2

50.9 M	0.0	3.824 CM					
	0.0	0.731 MR	0.224				
	0.0	2.273 CM	0.0	0.0			
	0.0	0.132 MR	0.0	0.0	0.228		
	0.0	0.137 CM	-0.993	-0.110	0.0	0.0	
	0.0	2.000 PC	0.228	1.000	0.0	0.0	-0.114

DRIFT 3.0 0.5000 M

51.4 M	0.0	3.833 CM					
	0.0	0.731 MR	0.233				
	0.0	2.275 CM	0.0	0.0			
	0.0	0.132 MR	0.0	0.0	0.231		
	0.0	0.137 CM	-0.992	-0.110	0.0	0.0	
	0.0	2.000 PC	0.237	1.000	0.0	0.0	-0.114

BEND 4.000 6.10000 M 4.800 KG 0.0000 (0.838 D)

LABEL = B2

57.5 M	0.0	3.991 CM					
	0.0	1.024 MR	0.358				
	0.0	2.295 CM	0.0	0.0			
	0.0	0.132 MR	0.0	0.0	0.264		
	0.0	0.193 CM	-0.980	-0.165	0.0	0.0	
	0.0	2.000 PC	0.362	1.000	0.0	0.0	-0.169

DRIFT 3.0 0.5000 M

58.0 M	0.0	4.010 CM					
	0.0	1.024 MR	0.369				
	0.0	2.296 CM	0.0	0.0			
	0.0	0.132 MR	0.0	0.0	0.266		

0.0	0.193 CM	-0.978	-0.165	0.0	0.0	
0.0	2.000 PC	0.373	1.000	0.0	0.0	-0.169

END* 4.000 3.05000 M 4.800 KG 0.0000 (0.419 D)

LABEL = B2

61.1 M	0.0	4.145 CM				
	0.0	1.170 MR	0.438			
	0.0	2.307 CM	0.0	0.0		
	0.0	0.132 MR	0.0	0.0	0.283	
	0.0	0.222 CM	-0.968	-0.197	0.0	0.0
	0.0	2.000 PC	0.441	1.000	0.0	0.0
						-0.202

DRIFT 3.0 1.0000 M

62.1 M	0.0	4.198 CM				
	0.0	1.170 MR	0.460			
	0.0	2.311 CM	0.0	0.0		
	0.0	0.132 MR	0.0	0.0	0.288	
	0.0	0.222 CM	-0.961	-0.197	0.0	0.0
	0.0	2.000 PC	0.464	1.000	0.0	0.0
						-0.202

QUAD 5.00 1.52000 M 1.6812 KG 5.000 CM (39.415 M)

VARY CODE = 020000

LABEL = Q3

63.6 M	0.0	4.201 CM				
	0.0	1.152 MR	-0.433			
	0.0	2.362 CM	0.0	0.0		
	0.0	0.646 MR	0.0	0.0	0.982	
	0.0	0.222 CM	-0.950	0.692	0.0	0.0
	0.0	2.000 PC	0.496	0.567	0.0	0.0
						-0.202

DRIFT 3.0 0.5000 M

64.1 M	0.0	4.176 CM				
	0.0	1.152 MR	-0.422			
	0.0	2.394 CM	0.0	0.0		
	0.0	0.646 MR	0.0	0.0	0.982	
	0.0	0.222 CM	-0.946	0.692	0.0	0.0
	0.0	2.000 PC	0.507	0.567	0.0	0.0
						-0.202

QUAD 5.00 1.52000 M 1.6812 KG 5.000 CM (39.415 M)

VARY CODE = 020000

LABEL = Q3

65.6 M	0.0	4.025 CM				
	0.0	1.846 MR	-0.810			
	0.0	2.537 CM	0.0	0.0		
	0.0	1.268 MR	0.0	0.0	0.996	
	0.0	0.222 CM	-0.933	0.967	0.0	0.0
	0.0	2.000 PC	0.540	0.056	0.0	0.0
						-0.202

DRIFT 3.0 0.5000 M

66.1 M	0.0	3.950 CM				
	0.0	1.846 MR	-0.802			
	0.0	2.600 CM	0.0	0.0		
	0.0	1.268 MR	0.0	0.0	0.996	
	0.0	0.222 CM	-0.928	0.967	0.0	0.0

0.0 2.000 PC 0.552 0.056 0.0 0.0 -0.202

QUAD 5.00 1.52000 M 1.6812 KG 5.000 CM (39.415 M)
 VARY CODE = 020000
 LABEL = Q3
 67.6 M

0.0 3.654 CM
 0.0 2.682 MR -0.896
 0.0 2.844 CM 0.0 0.0
 0.0 1.959 MR 0.0 0.0 0.999
 0.0 0.222 CM -0.910 0.999 0.0 0.0
 0.0 2.000 PC 0.589 -0.169 0.0 0.0 -0.202

DRIFT 3.0 1.5000 M
 69.1 M

0.0 3.299 CM
 0.0 2.682 MR -0.870
 0.0 3.138 CM 0.0 0.0
 0.0 1.959 MR 0.0 0.0 0.999
 0.0 0.222 CM -0.886 0.999 0.0 0.0
 0.0 2.000 PC 0.632 -0.169 0.0 0.0 -0.202

QUAD 5.00 1.52000 M -2.1236 KG 5.000 CM (-30.749 M)
 VARY CODE = 030000
 LABEL = Q4
 70.7 M

0.0 3.029 CM
 0.0 1.890 MR -0.648
 0.0 3.356 CM 0.0 0.0
 0.0 0.910 MR 0.0 0.0 0.995
 0.0 0.222 CM -0.853 0.950 0.0 0.0
 0.0 2.000 PC 0.683 0.114 0.0 0.0 -0.202

DRIFT 3.0 0.5000 M
 71.2 M

0.0 2.969 CM
 0.0 1.890 MR -0.629
 0.0 3.401 CM 0.0 0.0
 0.0 0.910 MR 0.0 0.0 0.996
 0.0 0.222 CM -0.840 0.950 0.0 0.0
 0.0 2.000 PC 0.700 0.114 0.0 0.0 -0.202

QUAD 5.00 1.52000 M -2.1236 KG 5.000 CM (-30.749 M)
 VARY CODE = 030000
 LABEL = Q4
 72.7 M

0.0 2.869 CM
 0.0 1.526 MR -0.088
 0.0 3.455 CM 0.0 0.0
 0.0 0.221 MR 0.0 0.0 -0.924
 0.0 0.222 CM -0.795 0.674 0.0 0.0
 0.0 2.000 PC 0.754 0.588 0.0 0.0 -0.202

DRIFT 3.0 0.5000 M
 73.2 M

0.0 2.863 CM
 0.0 1.526 MR -0.062
 0.0 3.445 CM 0.0 0.0
 0.0 0.221 MR 0.0 0.0 -0.924
 0.0 0.222 CM -0.779 0.674 0.0 0.0

0.0 2.000 PC 0.771 0.588 0.0 0.0 -0.202

QUAD 5.00 1.52000 M -2.1236 KG 5.000 CM (-30.749 M)

VARY CODE = 030000

LABEL = Q4

74.7 M

0.0 2.928 CM
 0.0 1.769 MR 0.541
 0.0 3.330 CM 0.0 0.0
 0.0 1.304 MR 0.0 0.0 -0.998
 0.0 0.222 CM -0.726 0.186 0.0 0.0
 0.0 2.000 PC 0.819 0.925 0.0 0.0 -0.202

DRIFT 3.0 25.0000 M

99.7 M

0.0 6.492 CM
 0.0 1.769 MR 0.925
 0.0 0.232 CM 0.0 0.0
 0.0 1.304 MR 0.0 0.0 -0.267
 0.0 0.222 CM -0.201 0.186 0.0 0.0
 0.0 2.000 PC 1.000 0.925 0.0 0.0 -0.202

TRANSFORM 1

-2.30875 -0.00000 0.0 0.0 0.0 3.24545
 -0.82921 -0.43313 0.0 0.0 0.0 0.81827
 0.0 0.0 -4.63859 -0.00000 0.0 0.0
 0.0 0.0 6.96382 -0.21558 0.0 0.0
 -0.08020 -0.14057 0.0 0.0 1.00000 -0.02242
 0.0 0.0 0.0 0.0 0.0 1.00000

FIT 10.0 -1. 2. 0.0 / 0.000

-0.000

LABEL = F2

FIT 10.0 -3. 4. 0.0 / 0.000

-0.000

LABEL = F2

DRIFT 3.0 25.0000 M

124.7 M

0.0 10.717 CM
 0.0 1.769 MR 0.973
 0.0 3.206 CM 0.0 0.0
 0.0 1.304 MR 0.0 0.0 0.998
 0.0 0.222 CM -0.045 0.186 0.0 0.0
 0.0 2.000 PC 0.987 0.925 0.0 0.0 -0.202

LENGTH 124.6997 M

TABLE 7
Required Quad Alignment Tolerances

Displacement Errors		
Type of Misalignment	Amount of misalignment for 3mm displacement of central ray at focal plane	Permissible relative misalignment for .5mm displacement
Horizontal displacement along x-axis	Q ₁ .86mm	.14mm
	Q ₂ .60	.10
	Q ₃ .98	.16
	Q ₄ 1.47	.24
Vertical displacement along y-axis	Q ₁ .96mm	.16mm
	Q ₂ 2.31	.38
	Q ₃ 4.11	.68
	Q ₄ 1.73	.29
Rotation about horizontal (x) axis through center	Q ₁ 30.mr	5.mr
	Q ₂ 24.	4.1
	Q ₃ 75.	12.5
	Q ₄ 113.	18.8
Rotation about vertical (y) axis through center	Q ₁ 2.9mr	.49mr
	Q ₂ 5.6	.93
	Q ₃ 16.1	2.7
	Q ₄ 8.3	1.4

TABLE 7 (continued)
QUAD ALIGNMENT TOLERANCES

Focussing Errors

Type of Misalignment		Amount of Misalignment for:		
		.05% $\Delta p/p$.15mr $\Delta \theta_y$	5mr $\Delta \theta_x$
\int Bdl error,	Q_1	<u>.31%</u> = .18 KG-m	.70 KG-m	1.7 ⁴ KG-m
	Q_2	<u>.30%</u> = .10 KG-m	1.0 KG-m	1.0 KG-m
	Q_3	<u>.61%</u> = .12 KG-m		
	Q_4	<u>1.0 %</u> = .32 KG-m		
Quad field error, all quads high		<u>.31%</u>	1.5%	5.0%
	Q_1 high	1.2%	<u>1.1%</u>	11.5%
	Q_2 high	.36%	<u>.33%</u>	3.6%
	Q_3 high	<u>.49%</u>		
	Q_4 high	<u>2.2 %</u>		
Quad rotation about x-axis	Q_1	2.3mr	15mr	23mr
	Q_2	<u>2.3</u>	15	23
	Q_3	<u>3.8</u>		
	Q_4	<u>3.8</u>		
Quad displacement along z-axis	Q_1	<u>2.8cm</u>		
	Q_2	<u>2.5cm</u>		
	Q_3	<u>6.9cm</u>		
	Q_4	<u>7.7cm</u>		

TABLE 8

Transfer matrices to decode planes and the decode algorithms
for 200 GeV spectrometer

Horizontal Decode Planes

Units are cms, %, milliradians

Decode planes #H1 at middle of last quad pair.

	x_o	θ_o	y_o	ϕ_o	z_o	δ
x	0.63103	<u>2.47299</u>	0.0	0.0	0.0	0.96019
θ	-1.07076	-2.61159	0.0	0.0	0.0	-0.16521
y	0.0	0.0	-11.62762	0.36427	0.0	0.0
ϕ	0.0	0.0	-8.12152	0.51767	0.0	0.0
z	-0.09239	-0.20991	0.0	0.0	1.00000	-0.02052
δ	0.0	0.0	0.0	0.0	0.0	1.00000

Decode plane #H2 at momentum focus.

	x_o	θ_o	y_o	ϕ_o	z_o	δ
x	-1.46121	0.00001	0.0	0.0	0.0	<u>3.06713</u>
θ	-0.67540	-0.68436	0.0	0.0	0.0	0.78543
y	0.0	0.0	-2.76759	-0.00000	0.0	0.0
ϕ	0.0	0.0	3.95957	-0.36132	0.0	0.0
z	-0.09239	-0.20991	0.0	0.0	1.00000	-0.02052
δ	0.0	0.0	0.0	0.0	0.0	1.00000

Decode plane #H3 at end of system (redundant).

	x_o	θ_o	y_o	ϕ_o	z_o	δ
x	-3.14970	-1.71088	0.0	0.0	0.0	5.03077
θ	-0.67540	-0.68436	0.0	0.0	0.0	0.78543
y	0.0	0.0	7.13134	-0.90330	0.0	0.0
ϕ	0.0	0.0	3.95957	-0.36132	0.0	0.0
z	-0.09239	-0.20991	0.0	0.0	1.00000	-0.02052
δ	0.0	0.0	0.0	0.0	0.0	1.00000

Horizontal Decode algorithms

1st Order Approximations:

$$\delta = \frac{(H2)}{3.067} \quad \%$$

$$\theta_o = \frac{(H1) - 0.31 (H2)}{2.47} \quad \text{Milliradians}$$

x_o = is assumed to be 0.05 cms or less

2nd Order corrected valued for the momentum:

$$\delta_{\text{corrected}} = \delta (1 - 0.06 \theta_o)$$

Convention. (H1) is coordinate of displacement of particle orbit in cms on #H1 plane.

Vertical Decode Planes

Units are cms, %, milliradians

Decode plane #V1. After last quad pair.

	x_o	θ_o	y_o	ϕ_o	z_o	δ
x	0.22728	1.71090	0.0	0.0	0.0	1.10360
θ	-0.67540	-0.68436	0.0	0.0	0.0	0.78543
y	0.0	0.0	-12.66653	0.90330	0.0	0.0
ϕ	0.0	0.0	3.95957	-0.36132	0.0	0.0
z	-0.09239	-0.20991	0.0	0.0	1.00000	-0.02052
δ	0.0	0.0	0.0	0.0	0.0	1.00000

TABLE 8 (continued)

Decode plane #V2. At momentum focus (redundant).

	x_o	θ_o	y_o	ϕ_o	z_o	δ
x	-1.46121	0.00001	0.0	0.0	0.0	3.05718
θ	-0.67540	-0.68436	0.0	0.0	0.0	0.78543
y	0.0	0.0	-2.76759	-0.00000	0.0	0.0
ϕ	0.0	0.0	3.95957	-0.36132	0.0	0.0
z	-0.09239	-0.20991	0.0	0.0	1.00000	-0.02052
δ	0.0	0.0	0.0	0.0	0.0	1.00000

Decode plane #V3. At end of system.

	x_o	θ_o	y_o	ϕ_o	z_o	δ
x	-3.14970	-1.71038	0.0	0.0	0.0	5.03077
θ	-0.67540	-0.68436	0.0	0.0	0.0	0.78543
y	0.0	0.0	<u>7.13134</u>	<u>-0.90330</u>	0.0	0.0
ϕ	0.0	0.0	3.95957	-0.36132	0.0	0.0
z	-0.09239	-0.20991	0.0	0.0	1.00000	-0.02052
δ	0.0	0.0	0.0	0.0	0.0	1.00000

Vertical Decode algorithms

1st Order Approximations:

$$y_o = - \left[\frac{(V1) + (V3)}{5.53} \right]$$

$$\phi_o = - \left[\frac{(V1) + 1.77 (V3)}{0.69} \right]$$

2nd Order corrected value for ϕ_o :

$$\phi_o \text{ corrected} = \phi_o \left[1 - .13 \delta \right]$$

TABLE 9

LIST OF MAGNETS AND THEIR COSTS*

Type	No.	Unit Lengths in Meters	Cost
N.A.L. B ₂ Magnets	3	6.1	\$ 36K
N.A.L. Bend Magnets	2	3.05	14K
Quads 4Q60	14	1.52	112K
N.A.L. Bends for beam Deflection System	4	3.05	28K
Sub-Total.			<u>\$190K</u>
Power supplies for Quads ⁺			42K
Power supplies for Bends ⁺			<u>44K</u>
Sub-Total.			<u>\$ 86K</u>
Sub-Total			\$276K
+ Dies, fixtures, tooling for 4Q60			20K
+ 25% for installation, cabling			<u>75K</u>
GRAND TOTAL.			<u><u>\$371K</u></u>

* Based on estimates from the N.A.L. main ring group.

TABLE 10
University Responsibilities

ITEM	UNIVERSITY GROUP RESPONSIBLE
DISC Cerenkov Counters	C.E.R.N.
Differential Counters	Stanford Group
Trigger Counters and Fast Elec. and Cabling	M.I.T., Brown Univ.
Threshold Cerenkov's	A.N.L.
Magnetic Measurements	Stanford
Charpak Chambers	Cornell, Univ. of Bari
Preprocessor and Encoder and Interfacing	Cornell, Univ. of Bari
Software for Computer	M.I.T.
Mechanical Slits, Beam Instrumentation. Monitors and Beam Hodoscopy	C.E.R.N., Stanford, and A.N.L.
Coplanarity. Hodoscope (side arm scintillators)	Stanford, N.E. Univ.
Coordination	Stanford

This Table is based on the assumption that the various University Groups will continue to be funded next year at the same level as this year. In addition, funds have been requested by the Stanford University Group from the A.E.C. and by the Cornell Group from either the A.E.C. or N.S.F. for this experiment.

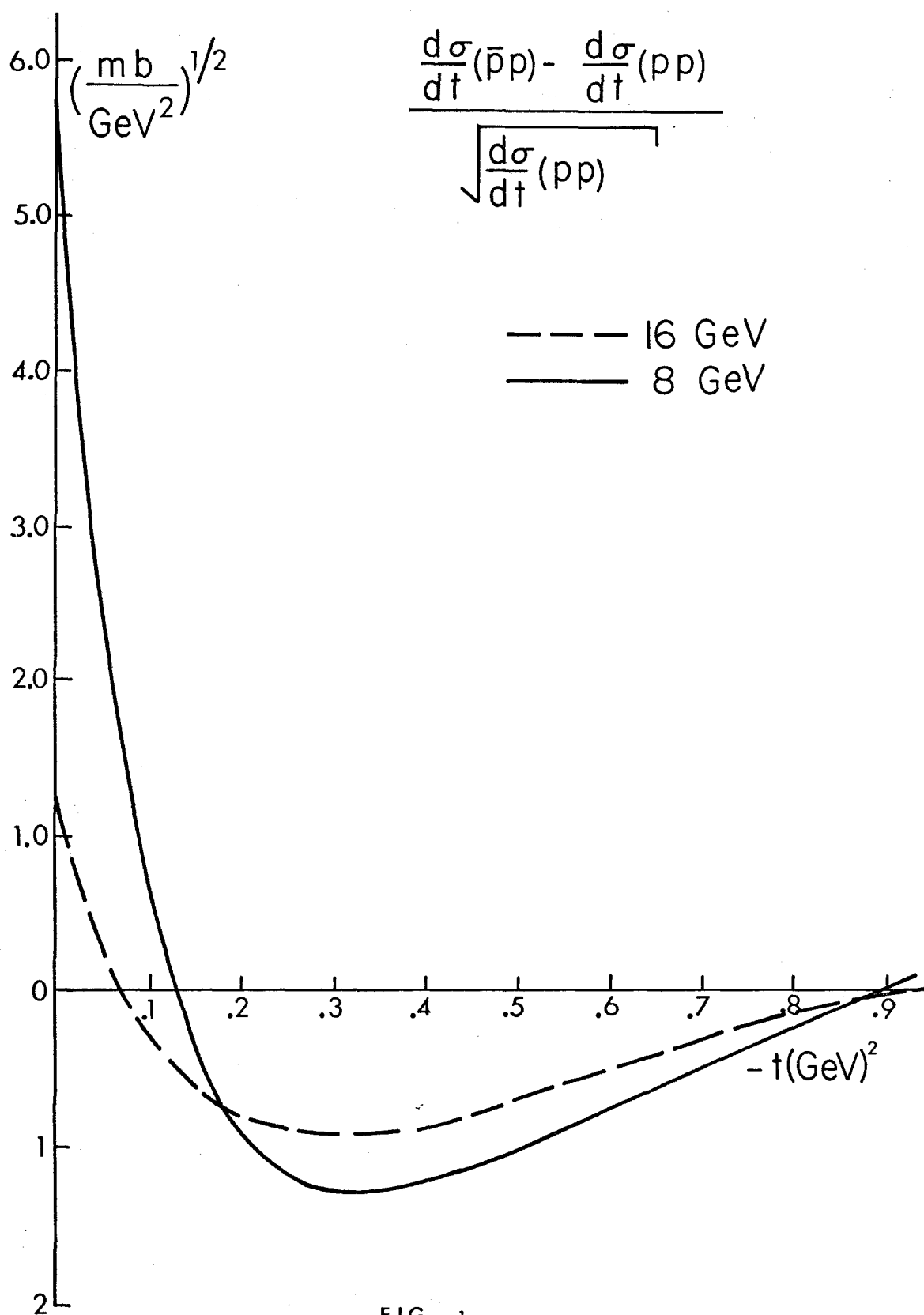
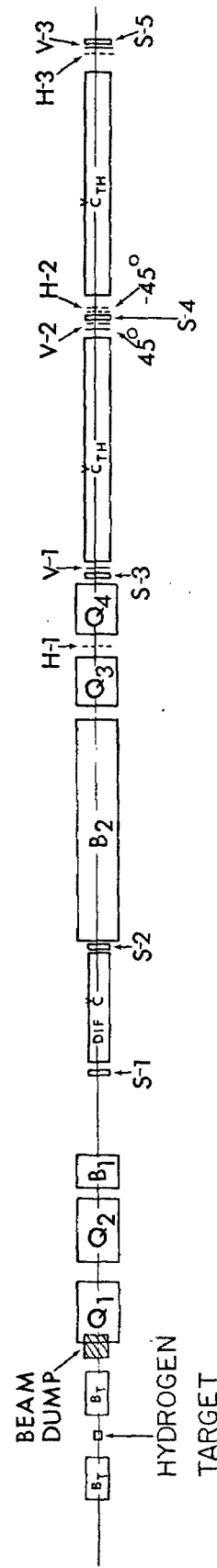


FIG. 1

FIG. 2
200 GeV/c SPECTROMETER
LAYOUT



LEGEND

- B BEND MAGNET
- Q QUADRUPOLE
- DIF DIFFERENTIAL CERENKOV COUNTER
- C SCINTILLATION COUNTER
- S HORIZONTAL WIRE PLANE
- H VERTICAL WIRE PLANE
- V 45° WIRE PLANE
- 45° -45° WIRE PLANE

SCALE IN METERS

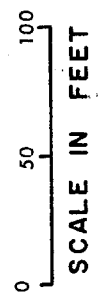
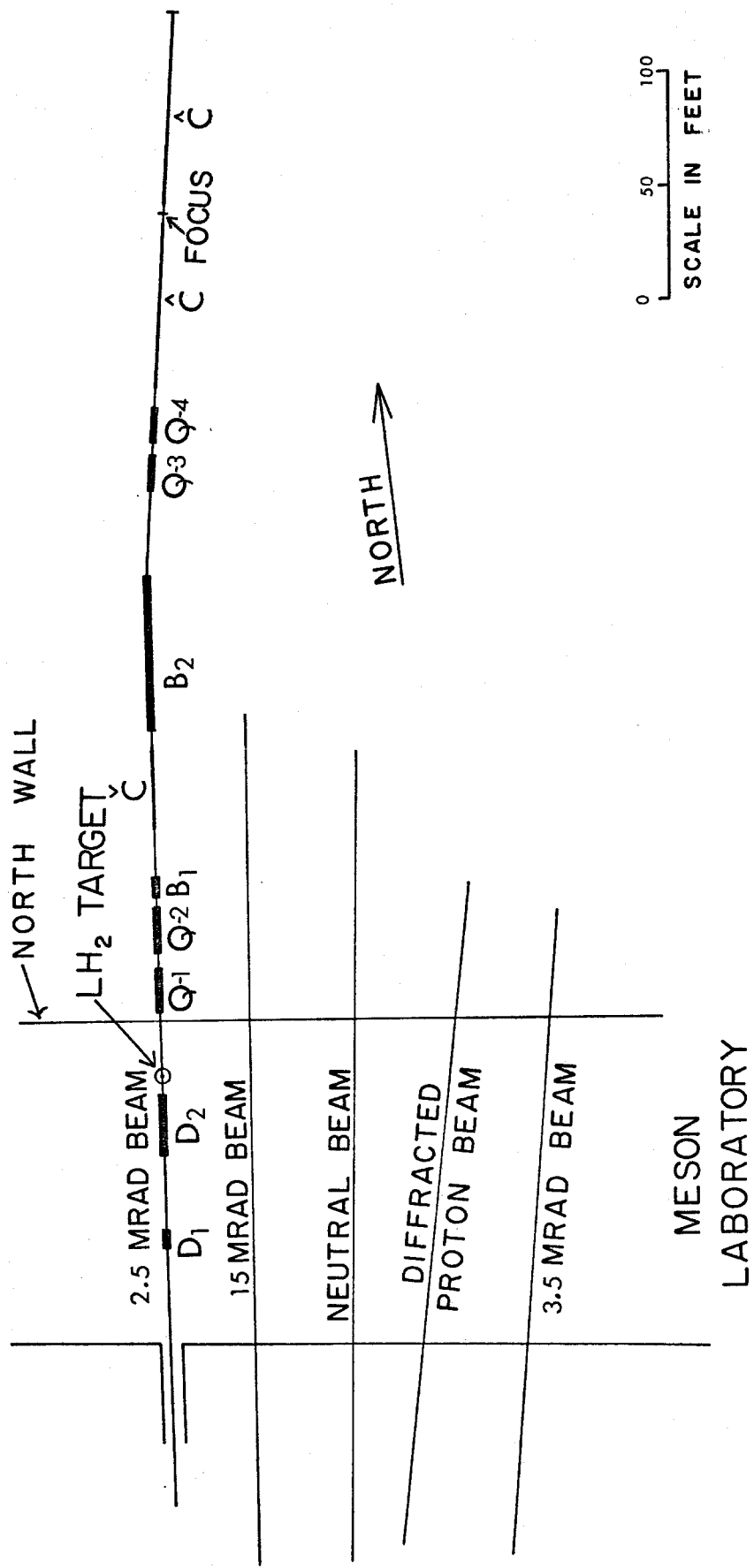
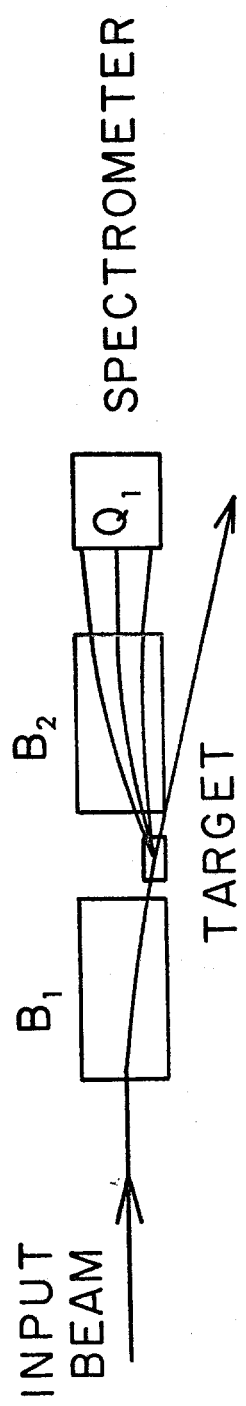


FIG. 3
PLAN VIEW OF 200 GeV/c SPECTROMETER

FIG. 4A
MAGNETIC VARIATION OF SCATTERING
ANGLE

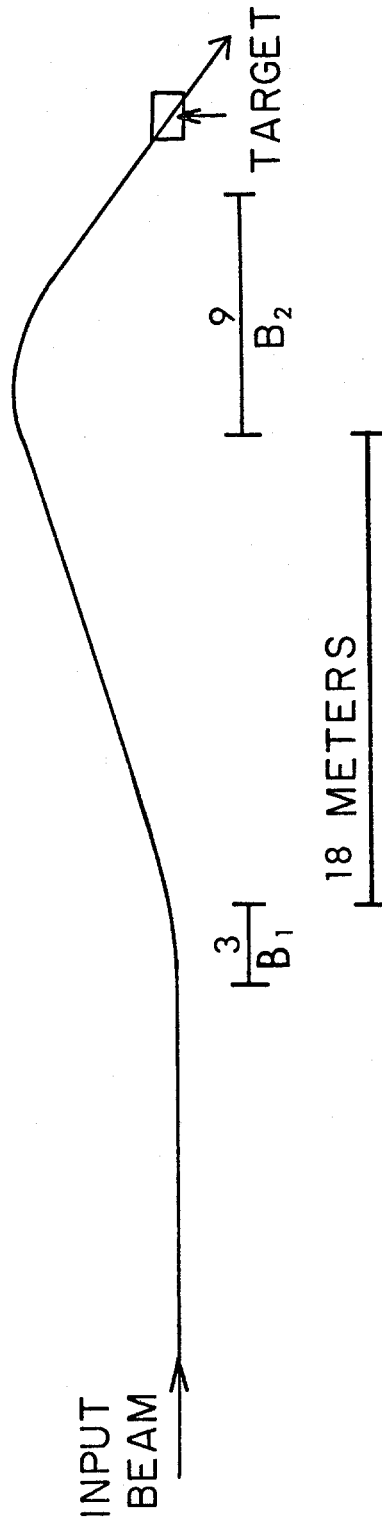


3 METERS
└───┘
HORIZ. SCALE
[4 INCHES]
VERT. SCALE

SCHEME A

FIG. 4B

MAGNETIC DEFLECTION



SCHEME B

APPENDIX 1DIFFERENTIAL ACHROMATIC CERENKOV (DISC)
COUNTER FOR NAL 200 GeV BEAMS

1. The number of protons produced by Čerenkov radiation is

$$\frac{dN}{dK} = 2\pi L \alpha \sin^2 \theta \quad K = \frac{1}{\lambda}.$$

With the best phototubes, the accepted light-band ($2200 < \lambda < 5000 \text{ Å}$, $\Delta K = 2.5 \times 10^4 \text{ cm}^{-1}$) has an average efficiency $\bar{\epsilon} = 0.07$, taking into account the losses in the optical system of a DISC (see Duteil, et.al, CERN, 68-14). The total number of photoelectrons per unit length is then

$$\frac{N}{L} = 2\pi \alpha \Delta K \bar{\epsilon} \theta^2 = 80 \theta^2 \text{ electrons cm}^{-1}.$$

If eight phototubes collect the light along the circumference, the average number of photoelectrons per tube \bar{N} must be such that the eightfold coincidence has a probability of occurring of at least 2/3, i.e.

$$(1 - e^{-\bar{N}})^8 = 0.66.$$

This gives $\bar{N} = 3.0$, $N = 8$, $\bar{N} = 24$, and for the length L of the Čerenkov counter

$$L = \frac{0.30}{\theta^2} \text{ cm.} \quad (1)$$

2. From the relation giving the Čerenkov angle

$$\cos \theta = \frac{1}{\beta n}$$

differentiation gives

$$\text{tg } \theta = \frac{d\beta}{\beta} + \frac{dn}{n}.$$

When dealing with high-energy particles

$$\gamma = \frac{E}{n} \gg 1, \quad \beta = \sqrt{1 - \frac{1}{\gamma^2}} = 1 - \frac{1}{2\gamma^2}$$

and small Čerenkov angles ($\theta \ll 1$), the index of refraction of the gas in the counter is close to unity ($n - 1 \ll 1$) and the first relation can be simplified:

$$\cos \theta = 1 - \frac{\theta^2}{2} = \frac{1}{\left(1 - \frac{1}{2\gamma^2}\right) [1 - (n - 1)]} = 1 - \left[(n - 1) - \frac{1}{2\gamma^2} \right]$$

which gives

$$(n - 1) = \frac{\theta^2}{2} \left[1 - \frac{1}{(\gamma\theta)^2} \right] \quad (2)$$

For a gas, the relation between n and the pressure P , in atmospheres, is

$$(n - 1)_P = (n - 1)_{P=1} \times P$$

and the pressure needed in the counter is

$$P = \frac{\theta^2}{2(n - 1)_{P=1}} \left[1 + \frac{1}{(\gamma\theta)^2} \right] \text{ atm.} \quad (3)$$

3. At fixed n , i.e., fixed gas pressure and temperature

$$\frac{d\beta}{\beta} = \theta \, d\theta.$$

At fixed energy (or momentum) E , two particles of mass m_1 and m_2 have

$$\Delta\beta = \frac{m_1^2 - m_2^2}{2E^2},$$

and in principle the separation of the two masses requires a circular slit which, after chromatic corrections, accepts light, satisfying the relation:

$$\theta \, \Delta\theta = \frac{m_1^2 - m_2^2}{2E^2}.$$

In practice, the effective separation, when the wanted particles (K-meson) are a small percentage of the unwanted ones (π meson),

must be at least three times as large, and the maximum energy resolved is given by the relation

$$\theta \Delta\theta = \frac{m_1^2 - m_2^2}{6E^2} \quad (4)$$

TABLE B-1

	$m_1^2 - m_2^2$
d-p	2.66 GeV ²
p-K	0.63 "
p- π	0.86 "
K- π	0.228 "
π -p	0.083 "

4. A practical lower limit for the angular width of the slit is

$$\Delta\theta = 10^{-4} = 0.1 \text{ mrad} = 20 \text{ sec. of arc.}$$

This represents also the maximum beam divergence accepted by the counters at maximum resolution.

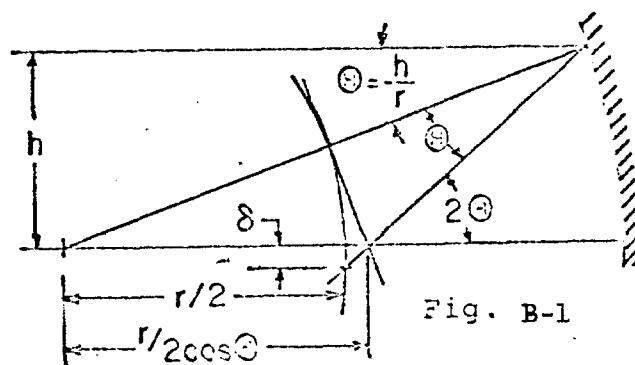
First let us see what is the limitation introduced by the aberration of the spherical mirror that focuses the Čerenkov light on the slit:

h = width of light beam

$r = 2f$ - radius of curvature

δ = spherical aberration

= width of image at focal plane



$$\delta = \left(\frac{r}{2 \cos \theta} - \frac{r}{2} \right) \cdot 2\theta = \frac{r}{2} \cdot \left(\frac{1}{\cos \theta} - 1 \right) \cdot \frac{2h}{r} = \left(1 + \frac{\theta^2}{2} - 1 \right) = \frac{h^3}{8f^2}$$

The confusion angle produced by spherical aberration is then

$$\Delta\theta_{\text{sph}} = \frac{\delta}{f} = \frac{h^3}{2f} \quad (5)$$

Since $h \approx 2f\theta$, $\Delta\theta_{\text{sph}} = \theta^3$, and the condition

$$\Delta\theta_{\text{sph}} < 10^{-4}$$

gives as an upper limit for the Čerenkov angle

$$\theta < 10^{-1.33} = 45 \text{ mrad},$$

a condition not difficult to meet in our case.

5. The chromatism of the Čerenkov radiation should be corrected because otherwise, at constant β , the resolution of Eq. (4) cannot be reached:

$$\theta \Delta\theta_{\text{chrom}} = \frac{\Delta n}{n} = \frac{\Delta n}{n-1} \cdot \frac{n-1}{n} = \frac{1}{V} (n-1) \quad (n \approx 1),$$

where $V = (n-1)/\Delta n$ is Abbe's number of the gas evaluated for a pair of wavelengths ($\lambda_1 = 2800$, $\lambda_2 = 4400$ Å) representative of the band accepted by the photomultipliers.

Using expression (2) one obtains

$$\Delta\theta_{\text{chrom}} = \frac{\theta}{2V} \left[1 + \frac{1}{(\gamma\beta^2)} \right]. \quad (6)$$

This equation also shows that the chromatic angle is not constant, but changes as γ changes.

TABLE B-2

Substance	$\dot{V} = (n - 1)/\Delta n$		$n - 1$ $\lambda = 3600$
	$\lambda_1 = 2800$	$\lambda_2 = 4400$	
SiO ₂	17.5		0.474
NaCl	9.2		0.580
KCl	8.3		0.524
H ₂	16.0		$1.44 \times 10^{-4} \times P$
He	55		$0.35 \times 10^{-4} \times P$
CO ₂	19.3		$4.62 \times 10^{-4} \times P$
A _{iv}	21.4		$3.01 \times 10^{-4} \times P$
SF ₆			$7.06 \times 10^{-4} \times P$

6. The chromatism of the Čerenkov light can in part be corrected with an axicon (i.e., a circular prism). In the original DISC, the axicon is composed of two elements glued together, one of SiO₂, the other of NaCl, that converge the blue and the ultraviolet light on the slit without any over-all deflection. For the large and long-focus mirrors needed at our energies it is possible to use a single SiO₂ element that, notwithstanding the slight over-all deviation of the light toward the axis, does not create any interference with the accepted beam.

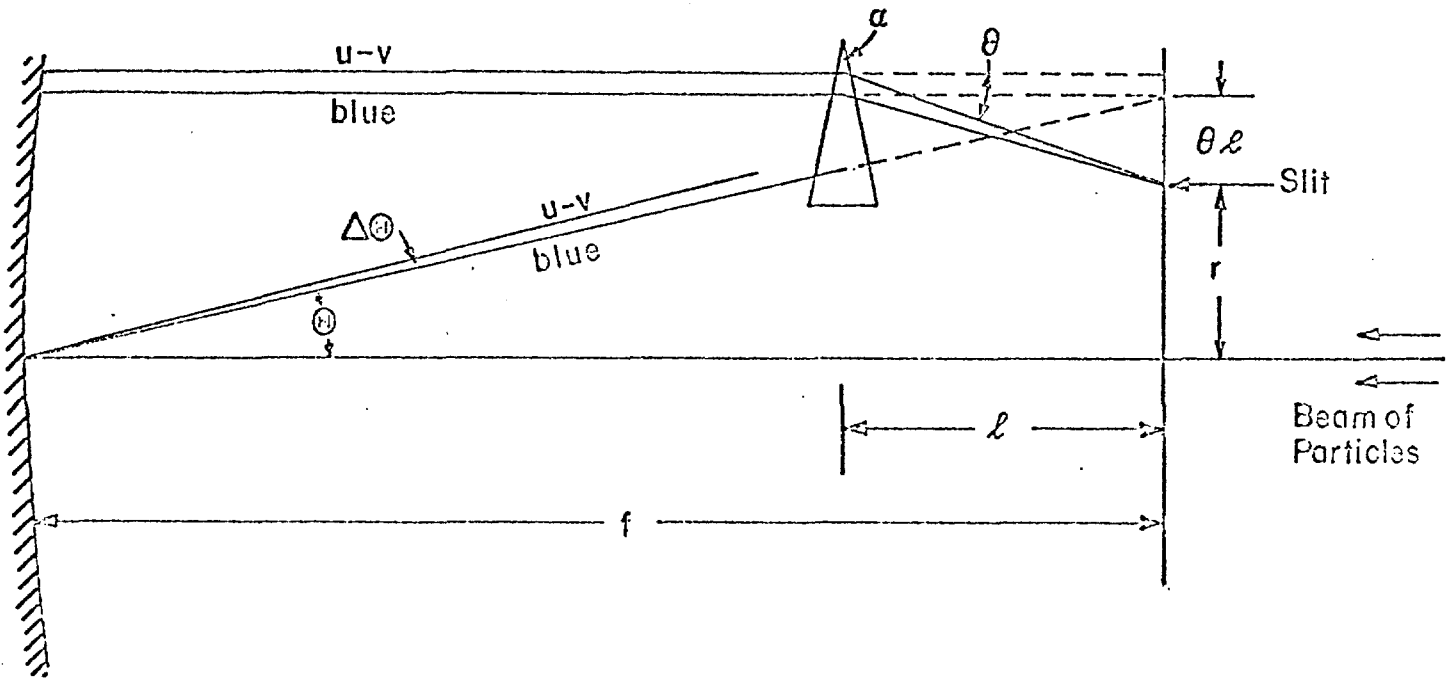


Fig. B-2.

For a prism at minimum deviation

$$n = \frac{\sin(\alpha + \theta)/2}{\sin \alpha/2} \quad \text{small angles} \quad 1 + \frac{\theta}{\alpha}, \quad \theta = \alpha(n - 1)$$

$$\frac{d\theta}{dn} = \frac{\alpha}{n - 1} \quad \text{and} \quad \Delta\theta = \alpha \frac{\Delta n}{n - 1} = \frac{\alpha(n - 1)}{V}$$

where $V = (n - 1)/\Delta n$ is the Abbe' number of the glass (see Table 2).

The achromatism is obtained when

$$\Delta\theta \, l = \Delta\theta_{\text{chrom}} f,$$

consequently

$$\alpha = \frac{V}{n - 1} \frac{f}{l} \Delta\theta_{\text{chrom}}$$

$$\theta = V \frac{f}{l} \Delta\theta_{\text{chrom}}.$$

(7)

Since $\Delta\theta_{\text{chrom}}$ depends on γ [Eq. (6)] once α is fixed, when γ changes, l should be changed in order to satisfy Eq. (7). In that case also θ changes, and since the radius of the circular slit r is fixed, the change of l implies a slight change of θ , the Čerenkov angle.

In practice, a fixed position of the prism could be satisfactory over a limited range of γ , and this is the solution described below.

7. Example for the 200 GeV beam

The most demanding doublet is $K\pi$, and Table 3 shows the values of $\theta\Delta\theta$ needed.

TABLE B-3

Energy (GeV)	$\theta\Delta\theta$ for $K - \pi$ [Eq. (4)]
200	0.95×10^{-6}
180	1.15×10^{-6}
150	1.70×10^{-6}
100	3.8×10^{-6}

The instrument can be optimized for 150 GeV K mesons ($\gamma = 300$). Then $\theta\Delta\theta = 1.7 \times 10^{-6}$. With $\Delta\theta = 10^{-4}$, $\theta = 17$ mrad, and [Eq. (1)], the length of the counters is $L = 0.3/\theta^2 = 10^3$ cm = 10 m. These parameters determine all the others given in Table 4.

When particles with γ different from 300 are analyzed, the chromatism is not fully corrected. However, provided

Čerenkov angle.....	$\theta = 1.7 \times 10^{-2} = 17 \text{ mrad}$
Slit aperture	$\Delta\theta = 10^{-4} = 0.1 \text{ mrad}$
Slit width.....	$f\Delta\theta = 1.0 \text{ mm}$
Focal length of mirror $f = L$	$f = 10^3 \text{ cm} = 10 \text{ m}$
Diameter of accepted beam.....	$2\rho = 10 \text{ cm}$
Diameter of mirror $= 2\rho + 20f$	$2R = 44 \text{ cm}$
Chromatism of Čerenkov light $\gamma = \infty$	$\Delta\theta_{\text{chrom}} = 3.97 \times 10^{-4}$
[Eq. (6)] for air $\rightarrow \gamma = 300$	$\Delta\theta_{\text{chrom}} = 4.12 \times 10^{-4}$
Distance of prism from focal plane.....	$\lambda = f/10 = 10^2 \text{ cm}$
Height of light beam on mirror $= \theta f + 2\rho$	$h = 27 \text{ cm}$
Minimum height of prism $= h \lambda/f$	$h_m = 2.7 \text{ cm}$
Central radius of axicon $\theta(f - \lambda)$	$\delta = 15.3 \text{ cm}$
Angle of SiO prism [Eq. (7)].....	$\alpha = 0.152 = 8.75^\circ$
Mean deviation produced by prism.....	$\theta = 0.072 = 4.15^\circ$
Distance of slit from axis $= \theta f - 0\lambda$	$r = 98 \text{ mm}$
Air pressure $\gamma = \infty; 1 + 1/(\gamma\theta)^2 = 1.0000$	$P = 0.478 \text{ atm}$
[Eq. (3)] $\gamma = 300$	0.496
$\gamma = 200$	0.520
$\gamma = 100$	0.643
$\gamma = 50$	1.140
$\gamma = 100$: Chromatism of Čerenkov light.....	$\Delta\theta'_{\text{chrom}} = 5.35 \times 10^{-4}$
Width of beam at focal plane.....	$f(\Delta\theta' - \Delta\theta) = 1.23 \text{ mm}$
$\gamma = 50$: Chromatism of Čerenkov.....	$\Delta\theta''_{\text{chrom}} = 9.5 \times 10^{-4}$
Width of beam.....	$f(\Delta\theta'' - \Delta\theta) = 5.4 \text{ mm}$

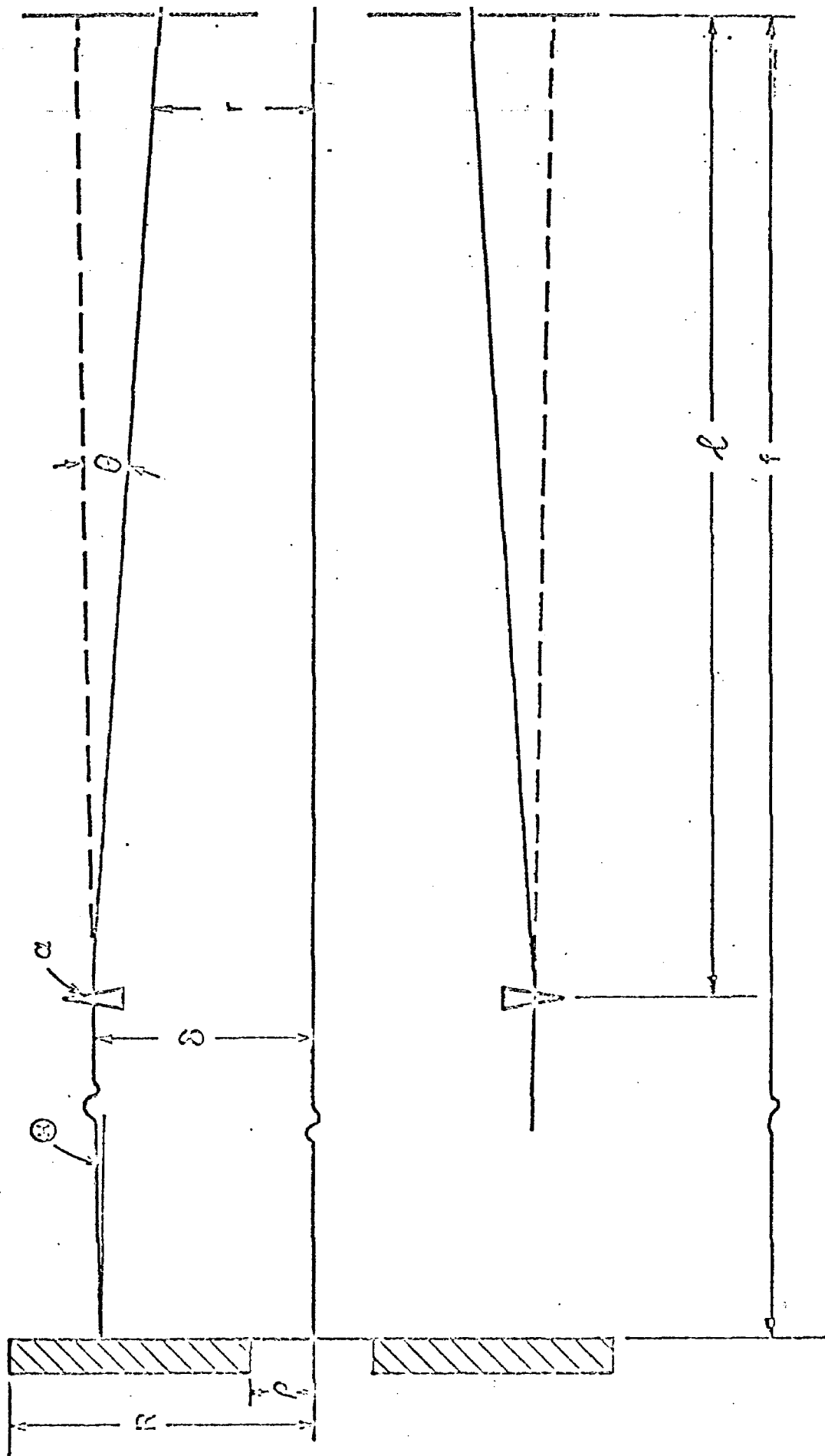


Fig. B-3

$\gamma > 100$, the resolution of the instrument remains almost unchanged, as can be seen from the example given in the table.

At $\gamma = 50$, the Čerenkov light is distributed, at the focal plane, over a ring ~ 6 mm wide and the slit should be opened accordingly. This is the case for 50 GeV protons (or antiprotons), but then the pK doublet is separated at the focus by 74 mm. $\gamma \approx 50$ should be considered the lowest value of γ at which the instrument can be useful.

8. Comments on the proposed center

a) The alignment of the counter within 0.1 mrad is delicate.

Also, the particle beams should be of adequate quality.

These requirements, however, should be met for any high-resolution DISC, independent of its length.

b) The great length implies a rather large mirror ($2R \approx 50$ cm) of long radius of curvature ($2f = 20$ m), and a structure of adequate rigidity.

c) The gas pressure inside the counter, never greater than a few PSI above atmospheric pressure, only demands a container that can be evacuated. It allows thin (10 cm) windows for the beam. It is also possible to use the phototubes without any window in front, a gain in light collection.

d) The width of the slit should be adjustable from the outside, over a range from 1-6 mm. It is the only movable part of the counter. The light collection after the slit can be helped by mirrors and light guides. It is assumed that all of the light eventually reaches the eight phototubes.

e) At fixed β (or γ , or E), $dn/n = \Delta n \approx 10^{-5}$. This implies that the index of refraction of the gas inside the counter can be measured and monitored with a precision $dn/n \approx 10^{-8}$, if reproducibility is wanted. A refractometer placed inside the counter itself is necessary, to avoid pressure and temperature differences. The refractometer used by Meunier et.al., consisting of an interferometer with a laser beam and an electronic system reading the number of fringes, performed very well and seems to provide the best solution. Unless it can be found on the market, this part of the project constitutes by itself a serious enterprise.

f) Astigmatism of the prism: only the central ray crosses the prism at minimum deviation, θ . Rays coming from the extreme of the light cone, i.e., at an angle $\Delta\phi = \theta/2$ to the central ray, are deflected by $\theta + \Delta\theta$:

$$\Delta\theta = \Delta\phi \left[\frac{\partial\theta}{\partial\phi} + \frac{\Delta\phi^2}{2} \frac{\partial^2\theta}{\partial\phi^2} \right]$$

$\partial\theta/\partial\phi = 0$ at minimum deviation (See Born and Wolf, p. 178).

$$\frac{\partial^2\theta}{\partial\phi^2} = 2 \operatorname{tg}\phi \left[1 - \frac{\operatorname{tg}^2\psi}{\operatorname{tg}^2\phi} \right] \frac{1}{\phi = n\psi \approx \alpha/2 \ll 1} \approx \left[1 - \frac{1}{n^2} \right]$$

and, at the focal plane, the width of the image due to prism astigmatism is

$$\Delta r_{\text{ast}} = 2\Delta\theta = \frac{1}{8} \theta^2 \approx \left[1 - \frac{1}{n^2} \right]$$

With the figures of Table 4 one obtains

$$\Delta r_{\text{ast}} = 2.9 \times 10^{-4} \text{ cm} = 2.9 \times 10^{-3} \text{ mm.}$$

a completely negligible quantity compared with the 1 mm minimum width of the slit.

This is true, however, only for particles moving along the optical axis.

Off-axis particles give rise to astigmatism that for an axicon can become serious. This point should be analyzed more deeply.

According to Meunier, a solution involving not an axicon but a curved-face corrector (a lens with a hole) could be more advantageous and simpler to build.

APPENDIX 2

DIFFERENTIAL CERENKOV COUNTER FOR THE PROPOSED 200 BeV SPECTROMETER

We consider the properties of a focussing Cerenkov counter of the type sketched in the figure. This design incorporates a positive veto for light outside the allowed Cerenkov cone.

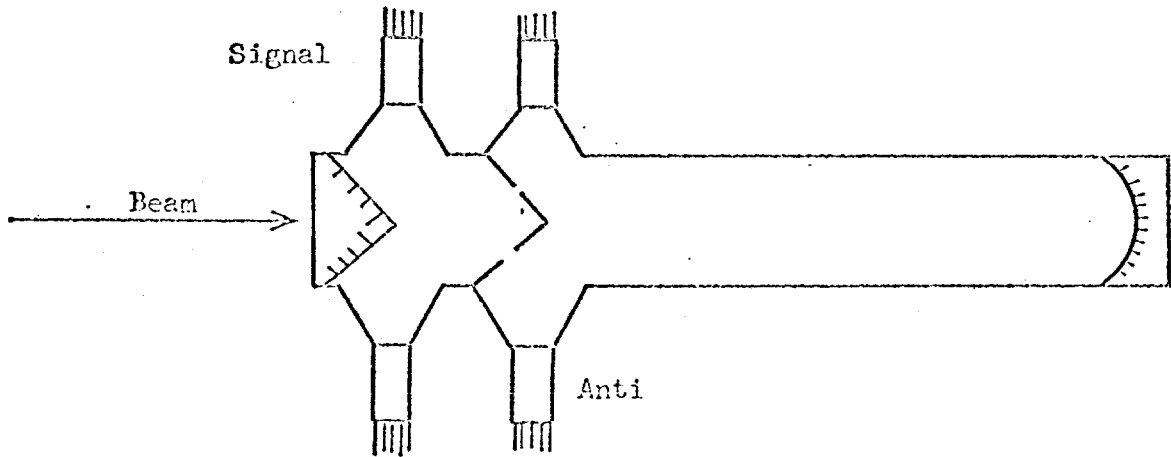


Fig. 1

The inner ring is therefore sufficiently well defined using one or two phototubes. With the tubes in coincidence we will have a 95% efficient device with only 7.2 photoelectrons. This in turn allows us to use a small Cerenkov angle θ which leads to high resolution and reduces the chromatic aberrations. In fact using He as the gas no chromatic corrections will be necessary up to 200 GeV/c. Also the density of the He will be easy to determine within the required accuracy.

We propose to build such a device 10m long with a fixed Cerenkov angle at 6.5 mrad and an efficiency of about 95% using the coincidence mode. Without the coincidence requirement we will have efficiencies close to 100% which would allow us to reduce the Cerenkov angle even further. The counter will be able

to separate π 's from K's between 50 GeV/c and 300 GeV/c.

Counter Efficiency

The numbers of photoelectrons per cm is given by the well known formula:

$$\frac{dN_e}{dl} = 2 \pi \alpha \cdot \epsilon \cdot \left(\frac{1}{\lambda_1} - \frac{1}{\lambda_2} \right) \cdot \sin^2 \theta \quad (1)$$

Here λ_1, λ_2 are the cutoff wavelengths for the tube, θ the Cerenkov angle and ϵ the conversion efficiency from produced light to photoelectrons. For the phototubes we will be using selected 58DUVP is with an average quantum efficiency of 25% between 2200 Å and 5000 Å. Assuming a loss of 10% for each reflection and 20% in absorption and general losses we have:

$$\frac{dN_e}{dl} = 170 \theta^2 \frac{\text{photoelectrons}}{\text{cm}}$$

$$\bar{N} = 170 \cdot l \cdot \theta^2$$

The coincidence efficiency $\eta = (1 - e^{-\bar{N}})^2$ is assumed to be 95% corresponding to $2\bar{N} = 7.2$ photoelectrons. For a Cerenkov counter 10m long, this leads to $\theta = 6.5$ mrad.

π -K Separation

The most critical particles to separate are K's from π 's. For a given index of refraction we have $\frac{d\beta}{\beta} = \theta \cdot d\theta$. The difference in β for π 's and

⁺Yu. P. Gorin et al., IHEP Prepring 69-63. Their measured threshold curves corresponds to a yield of $= 160 \cdot l \cdot \theta^2$. This value is used by H. Weisberg, E. Beier, D. Kreinick-N.A.L. Proposal No. 52. Reducing the yield to $100 \theta^2 l$ will make no appreciable change in the design.

K's of the same momentum is given by:

$$\Delta\beta = \frac{m_1^2 - m_2^2}{2E^2} = \frac{.228}{2E^2} \quad (2)$$

$$\theta d\theta = \frac{.228}{2E^2}$$

Since the counter vetos the unwanted particle, we only have to require that most of its light is reflected into the outer ring and only a small fraction into the inner ring. We will therefore assume that Eq. 2 gives a sufficient separation. In Table I the separation between π 's and K's is listed for several incident momenta, together with the spread in angles caused by the chromatic aberrations $\Delta\theta_{CH}$, the multiple scattering $\Delta\theta_S$, and the spectrometer optics $\Delta\theta_H$, $\Delta\theta_V$.

Table I

P (GeV/c)	$\theta_\pi - \theta_K$ mrad	$\Delta\theta_{CH}$ mrad	$\Delta\theta_S$ mrad	$\pm \Delta\theta_V$ mrad	$\pm \Delta\theta_H$ mrad	$\Delta\Omega$ μsr	Pressure atm
50	7.01	.194	.067	.220	.040	120.0	2.03
100	1.75	.094	.034	.157	.028	60.0	.96
150	.785	.0746	.022	.128	.024	40.0	.76
200	.438	.0678	.017	.111	.020	30.0	.69
250	.280	.0647	.013	.089	.018	19.2	.66
300	.195	.0630	.011	.074	.017	13.3	.64
350	.143	.0619	.010	.063	.015	9.8	.63
400	.110	.0613	.008	.055	.013	7.5	.62

It is clear that the counter separates π 's and K's up to 200-300 GeV without problems. To extend the counter beyond this point it is probably advantageous to correct for the chromatic aberrations in a standard way. The largest contribution to the spread in angles is then from the vertical angle of the incident beam $\Delta\theta_V$ which is approximately a factor of four larger than the $\Delta\theta_H$. The Cerenkov light for different θ_V then gets focussed as indicated in Fig. 2 for $\Delta\theta_H = 0$.

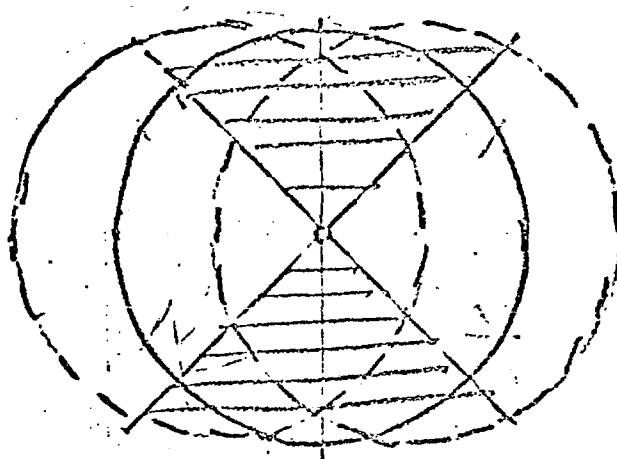


Fig. 2

By only accepting light within the crosshatched area the uncertainty in $\Delta\theta$ due to the divergence will only be about .025. Of course the total light yield is now down by a factor of 2 making the device only 70% efficient. However this efficiency is easily determined, and can be compensated for by either making the device longer, or by not requiring a coincidence between the two tubes atmosphere. Assuming we control and measure the density to .1% the error in angle caused by this will be .0054 mrad.